



COMILLAS
UNIVERSIDAD PONTIFICIA

ICAI

GRADO EN INGENIERÍA EN TECNOLOGÍAS
INDUSTRIALES

TRABAJO FIN DE GRADO
AERODYNAMIC COMPARISON OF
AMR22 AND W07 FRONT WINGS

Autor: Javier Páez Arjona

Director: Kenneth Powell

Madrid

Declaro, bajo mi responsabilidad, que el Proyecto presentado con el título

Aerodynamic comparison of AMR22 and W07 front wings

en la ETS de Ingeniería - ICAI de la Universidad Pontificia Comillas en el

curso académico 2021/2022 es de mi autoría, original e inédito y

no ha sido presentado con anterioridad a otros efectos.

El Proyecto no es plagio de otro, ni total ni parcialmente y la información que ha sido

tomada de otros documentos está debidamente referenciada.

Fdo.: Javier Páez Arjona

Fecha: 05/04/2022

Autorizada la entrega del proyecto

EL DIRECTOR DEL PROYECTO

A handwritten signature in blue ink that reads "K. H. Powell". The signature is written in a cursive style and is contained within a light blue rectangular box.

Fdo.: Kenneth Powell Fecha: 18./04./2022

AUTORIZACIÓN PARA LA DIGITALIZACIÓN, DEPÓSITO Y DIVULGACIÓN EN RED DE PROYECTOS FIN DE GRADO, FIN DE MÁSTER, TESIS O MEMORIAS DE BACHILLERATO

1º. Declaración de la autoría y acreditación de la misma.

El autor D. Javier Páez Arjona

DECLARA ser el titular de los derechos de propiedad intelectual de la obra: Aerodynamic comparison of AMR22 and W07 front wings que ésta es una obra original, y que ostenta la condición de autor en el sentido que otorga la Ley de Propiedad Intelectual.

2º. Objeto y fines de la cesión.

Con el fin de dar la máxima difusión a la obra citada a través del Repositorio institucional de la Universidad, el autor **CEDE** a la Universidad Pontificia Comillas, de forma gratuita y no exclusiva, por el máximo plazo legal y con ámbito universal, los derechos de digitalización, de archivo, de reproducción, de distribución y de comunicación pública, incluido el derecho de puesta a disposición electrónica, tal y como se describen en la Ley de Propiedad Intelectual. El derecho de transformación se cede a los únicos efectos de lo dispuesto en la letra a) del apartado siguiente.

3º. Condiciones de la cesión y acceso

Sin perjuicio de la titularidad de la obra, que sigue correspondiendo a su autor, la cesión de derechos contemplada en esta licencia habilita para:

- a) Transformarla con el fin de adaptarla a cualquier tecnología que permita incorporarla a internet y hacerla accesible; incorporar metadatos para realizar el registro de la obra e incorporar “marcas de agua” o cualquier otro sistema de seguridad o de protección.
- b) Reproducir la en un soporte digital para su incorporación a una base de datos electrónica, incluyendo el derecho de reproducir y almacenar la obra en servidores, a los efectos de garantizar su seguridad, conservación y preservar el formato.
- c) Comunicarla, por defecto, a través de un archivo institucional abierto, accesible de modo libre y gratuito a través de internet.
- d) Cualquier otra forma de acceso (restringido, embargado, cerrado) deberá solicitarse expresamente y obedecer a causas justificadas.
- e) Asignar por defecto a estos trabajos una licencia Creative Commons.
- f) Asignar por defecto a estos trabajos un HANDLE (URL *persistente*).

4º. Derechos del Autor.

El autor, en tanto que titular de una obra tiene derecho a:

- a) Que la Universidad identifique claramente su nombre como autor de la misma
- b) Comunicar y dar publicidad a la obra en la versión que ceda y en otras posteriores a través de cualquier medio.
- c) Solicitar la retirada de la obra del repositorio por causa justificada.
- d) Recibir notificación fehaciente de cualquier reclamación que puedan formular terceras personas en relación con la obra y, en particular, de reclamaciones relativas a los derechos de propiedad intelectual sobre ella.

5º. Deberes del autor.

El autor se compromete a:

- a) Garantizar que el compromiso que adquiere mediante el presente escrito no infringe ningún derecho de terceros, ya sean de propiedad industrial, intelectual o cualquier otro.
- b) Garantizar que el contenido de las obras no atenta contra los derechos al honor, a la intimidad y a la imagen de terceros.
- c) Asumir toda reclamación o responsabilidad, incluyendo las indemnizaciones por daños, que pudieran ejercitarse contra la Universidad por terceros que vieran infringidos sus derechos e intereses a causa de la cesión.
- d) Asumir la responsabilidad en el caso de que las instituciones fueran condenadas por infracción

de derechos derivada de las obras objeto de la cesión.

6º. Fines y funcionamiento del Repositorio Institucional.

La obra se pondrá a disposición de los usuarios para que hagan de ella un uso justo y respetuoso con los derechos del autor, según lo permitido por la legislación aplicable, y con fines de estudio, investigación, o cualquier otro fin lícito. Con dicha finalidad, la Universidad asume los siguientes deberes y se reserva las siguientes facultades:

- La Universidad informará a los usuarios del archivo sobre los usos permitidos, y no garantiza ni asume responsabilidad alguna por otras formas en que los usuarios hagan un uso posterior de las obras no conforme con la legislación vigente. El uso posterior, más allá de la copia privada, requerirá que se cite la fuente y se reconozca la autoría, que no se obtenga beneficio comercial, y que no se realicen obras derivadas.
- La Universidad no revisará el contenido de las obras, que en todo caso permanecerá bajo la responsabilidad exclusiva del autor y no estará obligada a ejercitar acciones legales en nombre del autor en el supuesto de infracciones a derechos de propiedad intelectual derivados del depósito y archivo de las obras. El autor renuncia a cualquier reclamación frente a la Universidad por las formas no ajustadas a la legislación vigente en que los usuarios hagan uso de las obras.
- La Universidad adoptará las medidas necesarias para la preservación de la obra en un futuro.
- La Universidad se reserva la facultad de retirar la obra, previa notificación al autor, en supuestos suficientemente justificados, o en caso de reclamaciones de terceros.

Madrid, a 05 de Abril de 2022

ACEPTA: Javier Páez Arjona

Fdo

Motivos para solicitar el acceso restringido, cerrado o embargado del trabajo en el Repositorio Institucional:



COMILLAS
UNIVERSIDAD PONTIFICIA

ICAI

GRADO EN INGENIERÍA EN TECNOLOGÍAS
INDUSTRIALES

TRABAJO FIN DE GRADO
AERODYNAMIC COMPARISON OF
AMR22 AND W07 FRONT WINGS

Autor: Javier Páez Arjona

Director: Kenneth Powell

Madrid

Agradecimientos

Thanks to Pablo Hermoso Moreno, first in his class in the Aeronautical Engineering Degree at Imperial College London, Mercedes-AMG Petronas Formula One Team engineer during the 2018-2019 season, and current Machine Learning Consultant at AWS.

Thanks to Kenneth Powell, ScD aerospace engineer from MIT and currently a professor at the University of Michigan, director of this project.

To my parents for supporting me and offering me the opportunity to have exceptional academic training.

COMPARATIVA AERODINÁMICA DE LOS ALERONES DELANTEROS DEL AMR22 Y DEL W07

Autor: Páez Arjona, Javier.

Director: Powell Kenneth.

Entidad Colaboradora: ICAI

RESUMEN DEL PROYECTO

En este proyecto se ha desarrollado un estudio aerodinámico mediante Dinámica Computacional de Fluidos (CFD) de los alerones delanteros del W07, coche del equipo Mercedes de la temporada de 2016 de Formula 1 y el del AMR22, coche del equipo Aston Martin de la temporada de 2022 de Formula 1. El objetivo de este proyecto ha sido analizar cómo los sucesivos cambios de normativa realizados desde 2019 han variado las propiedades aerodinámicas de los alerones, al igual que la funcionalidad de estos.

Palabras clave: CFD, Carga Aerodinámica & Drag, Alerón Delantero, Cambio de Normativa, Aire Sucio, Funcionalidad.

1. Introducción

Los sucesivos cambios de normativa llevados a cabo por parte de la FIA desde 2019 han tratado de simplificar drásticamente la geometría del alerón delantero de los coches de Formula 1. El objetivo de disminuir la cantidad de aire sucio y así permitir un más fácil seguimiento entre los distintos monoplazas y, por lo tanto, ofrecer carreras más entretenidas, se ha llevado a su máxima expresión con los monoplazas de 2022.

2. Definición del proyecto

Es de todos estos cambios de normativa de donde surge el proyecto que se trata. Analizar los alerones delanteros de dos coches de antes y después de los cambios de normativa, el Mercedes W07 de 2016 y el Aston Martin AMR22 de 2022. Estudiar la efectividad del cambio de normativa a través de las propiedades aerodinámicas de los mismos.

3. Descripción del modelo/sistema/herramienta

Antes de llevar a cabo los cálculos, es necesario llevar a cabo una selección de los modelos o geometrías que se van a estudiar, teniendo en cuenta que estos nunca serán iguales que los modelos oficiales de los equipos ya que estos son confidenciales. Es por esto que, para la selección de los mismos se ha llevado a cabo un estudio de las diferencias entre el modelo y el real, eligiendo aquel cuyas diferencias afectasen menos al estudio.

Una vez elegidos los modelos a estudiar era necesario elegir el programa en el que se iban a realizar las simulaciones, siendo este el módulo Fluent del programa ANSYS. Posteriormente, era necesario definir los principales parámetros en los que se basa la tecnología de CFD: el volumen de control y el mallado del mismo.

Debido a la limitada potencia computacional, era necesario elegir tanto un volumen de control, como un mallado, lo suficientemente sofisticados como para obtener unos

resultados que pudiésemos considerar válidos, pero sin escoger un volumen de control ni un mallado que presenten problemas a la hora de la convergencia de las simulaciones.

Es por esto que se ha llevado a cabo con dos volúmenes de control: uno más grande, el cual presenta un mallado menos exhaustivo, y uno de dimensiones inferiores con un mallado más sofisticado. Se muestran los VC y el mallado del alerón en la Ilustración 1:

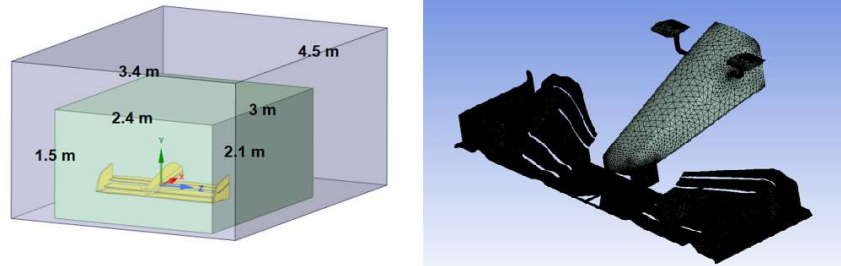


Ilustración 1: Volúmenes de Control y Mallado

Se ha utilizado una malla poliédrica volumétrica con las siguientes medidas: en el volumen de control más grande el tamaño de las celdas es de 500 mm, el tamaño de las celdas en el volumen de control menor es de 150 mm. El mallado del objeto de estudio tiene un mallado de 75 mm. Con respecto a la configuración del prism layer settings, se ha utilizado el método suavizado como el de variación entre los distintos mallados.

El flujo utilizado ha sido un flujo incompresible de aire que se encuentra en estado estacionario, es decir, con densidad y velocidad constante.

La convergencia en la ecuación de continuidad de las simulaciones se ha establecido para un valor menor de $10E-3$, lo cual ha resultado en 285 iteraciones para cada una de las simulaciones.

4. Resultados

Para un estudio más completo de los alerones, se han simulado los mismos a 4 velocidades diferentes: 25, 50, 75 y 100 m/s. Para cada una de las velocidades se ha obtenido la carga aerodinámica y la resistencia al aire. Se muestra en la Tabla 1 los valores para 50 y 75 m/s, es decir, 180 y 270 km/h, respectivamente, rango habitual de velocidades de un Formula 1.

	50 m/s			75 m/s		
	W07	AMR22	Difference	W07	AMR22	Difference
Carga Aerodinámica [N]	952,256	928,242	2,522%	2134,125	2083,390	2,377%
Resistencia al aire [N]	338,582	162,323	52,058%	762,507	365,874	52,017%

Tabla 1: Carga Aerodinámica y Resistencia al Aire para 50 y 75 m/s

Además, en la simulación de 75 m/s se han obtenido tanto las presiones sufridas por los alerones, como la velocidad del flujo de aire alrededor del mismo, el coeficiente de

presión de la sección del alerón y un estudio de los vórtices generados detrás de los mismos el cual se muestra en la Ilustración 2.

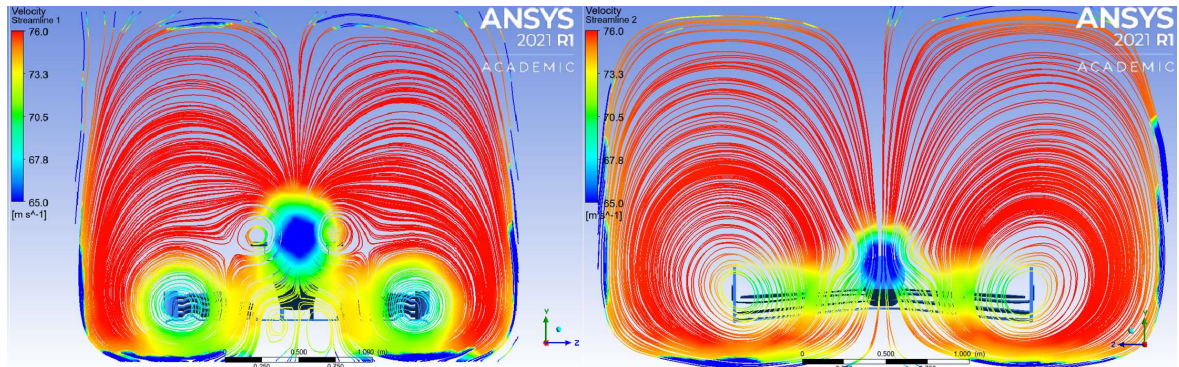


Ilustración 2: Vorticidad de W07 (←) y del AMR22 (→)

5. Conclusiones

Las principales conclusiones obtenidas a partir de los resultados es que, a pesar de una mayor simplificación en la geometría del alerón, este aumenta su propia eficiencia al mantener prácticamente constante la carga aerodinámica y reduciendo de forma considerable la resistencia al aire.

En cambio, analizando la Ilustración 2, se puede observar que el flujo de aire detrás del nuevo alerón se encuentra mucho más ordenado, cumpliendo así con los objetivos del cambio de normativa. Sin embargo, la complejidad de los vórtices generados por el alerón del W07 son responsables en gran parte de la carga aerodinámica generada por el resto del monoplaza.

Como conclusión, la funcionalidad entre ambos alerones es distinta para ambos alerones. El alerón del W07 genera carga aerodinámica por sí misma y también los vórtices que se crean en el mismo, generan gran parte de esta en el resto del coche. Sin embargo, como contrapartida a estos vórtices el alerón tiene que ser más vertical presentando así más resistencia al aire y genera más aire sucio. El alerón del AMR22 se presenta más simple, creando un flujo de aire más limpio detrás del mismo y es, el suelo y el difusor del coche a través del efecto suelo, el responsable de generar la carga aerodinámica que antes generaban los vórtices. Por tanto, los sucesivos cambios de normativa se muestran efectivos.

6. Referencias

- [1] Adrian Newey, director técnico y aerodinamicista de Red Bull Racing. “¿Cómo hacer un coche?”. Noviembre, 2017.
- [2] Greg Stuart. “10 things you need to know about the all-new 2022 F1 car”, F1 webpage. Julio, 2021. <https://www.formula1.com/en/latest/article.10-things-you-need-to-know-about-the-all-new-2022-f1-car.4OLg8DrXyzHzdoGrbqp6ye.html>
- [3] Simon McBeath. “Aerodinámica del automóvil de competición”. Febrero, 2013. P73-158.

AERODYNAMIC COMPARISON OF AMR22 AND W07 FRONT WINGS

Author: Páez Arjona, Javier.

Director: Powell Kenneth.

Collaborating Entity: ICAI

ABSTRACT

In this project, an aerodynamic study has been developed using Computational Fluid Dynamics (CFD) of the front wings of the W07, the car of the Mercedes team of the 2016 Formula 1 season, and that of the AMR22, the car of the Aston Martin team of the 2022 Formula 1 season. The objective of this project has been to analyze how the successive regulatory changes made since 2019 have varied the aerodynamic properties of the ailerons, as well as their functionality of these.

Keywords: CFD, Downforce & Drag, Front Wing, Change of Regulations, Dirty Air, Functionality.

1. Introduction

Successive regulatory changes carried out by the FIA since 2019 have sought to drastically simplify the geometry of the front wing of Formula 1 cars. The goal of reducing the amount of dirty air and thus allowing easier tracking between the different cars and, therefore, offering more entertaining races, has been taken to its maximum expression with the cars of 2022.

2. Project definition

It is from all these changes in regulations that the project in question arises. Analyze the front wings of two cars before and after the regulatory changes, the Mercedes W07 of 2016 and the Aston Martin AMR22 of 2022. Study the effectiveness of the change of regulations through the aerodynamic properties of the same.

3. Description of the model/system/tool

Before carrying out the calculations, it is necessary to select the models or geometries that are going to be studied, considering that these will never be the same as the official models of the teams since these are confidential. That is why, for the selection of the same, a study of the differences between the model and the real one has been carried out, choosing the one whose differences would affect the study the least.

Once the models to be studied were chosen, it was necessary to choose the program in which the simulations were going to be carried out, this being the Fluent module of the ANSYS program. Subsequently, it was necessary to define the main parameters on which CFD technology is based: the control volume and the meshing of the same.

Due to the limited computational power, it was necessary to choose both a control volume and a mesh, sophisticated enough to obtain results that we could consider valid,

but without choosing a control volume or a mesh that present problems when it comes to the convergence of the simulations.

That is why it has been made with two control volumes: a larger one, which has a less exhaustive meshing, and one of lower dimensions with a more sophisticated meshing. VCs and spoiler meshing are shown in Figure 1:

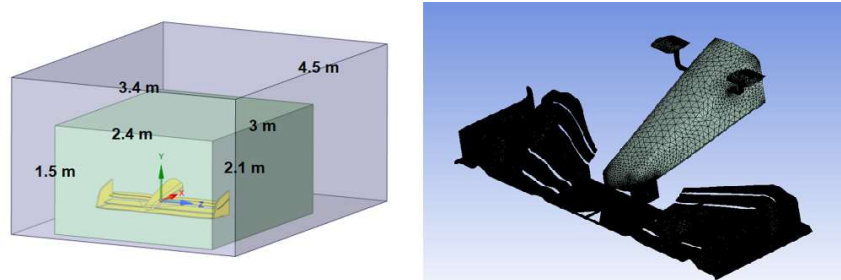


Figure 1: Control Volumes and Mesh

A volumetric polyhedral mesh with the following measurements has been used: in the largest control volume the size of the cells is 500 mm, and the size of the cells in the smaller control volume is 150 mm. The meshing of the object of study has a mesh of 75 mm. Concerning the configuration of the prism layer settings, the smoothed method has been used as the variation between the different meshes.

The flow used has been an incompressible flow of air that is in a steady-state, that is, with constant density and velocity.

Convergence in the continuity equation of the simulations has been established for a value less than $10E-3$, which has resulted in 285 iterations for each of the simulations.

4. Results

For a more complete study of the ailerons, they have been simulated at 4 different speeds: 25, 50, 75, and 100 m / s. For each of the speeds, downforce and air resistance have been obtained. values for 50 and 75 m/s, i.e., 180 and 270 km/h, respectively, the usual speed range of Formula 1 cars.

	50 m/s			75 m/s		
	W07	AMR22	Difference	W07	AMR22	Difference
Downforce [N]	952,256	928,242	2,522%	2134,125	2083,390	2,377%
Air resistance [N]	338,582	162,323	52,058%	762,507	365,874	52,017%

Table 1: Downforce and Air Resistance for 50 and 75 m/s

In addition, in the simulation of 75 m / s have been obtained both the pressures suffered by the ailerons, as well as the speed of the airflow around it, the pressure coefficient of the section of the spoiler, and a study of the vortices generated behind them which is shown in Figure 2.

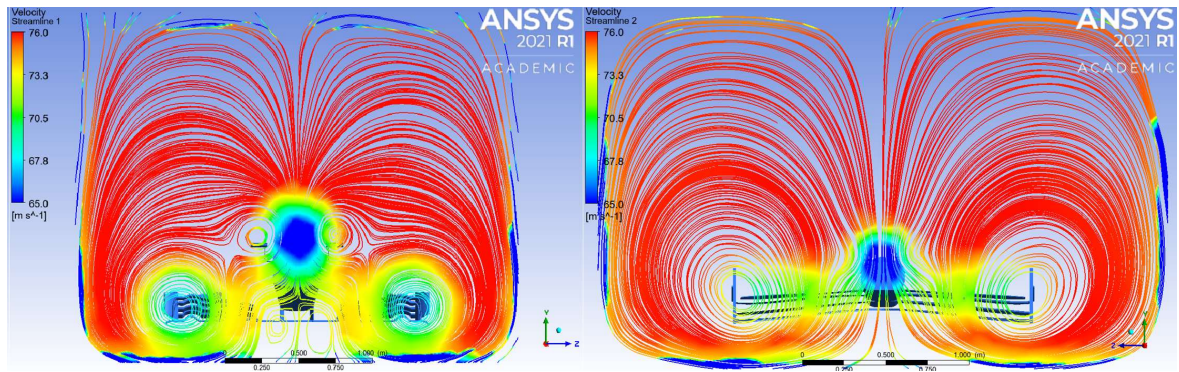


Figure 2: W07 (←) and AMR22 (→) Vorticity

5. Conclusions

The main conclusion obtained from the results is that, despite a greater simplification in the geometry of the spoiler, it increases its efficiency by keeping the downforce practically constant and considerably reducing air resistance.

On the other hand, analyzing Figure 2, it can be seen that the airflow behind the new spoiler is much more orderly, thus fulfilling the objectives of the regulatory change. However, the complexity of the vortices generated by the W07's spoiler is largely responsible for the downforce generated by the rest of the car.

In conclusion, the functionality of both ailerons is different for both ailerons. The spoiler of the W07 generates downforce by itself and also the vortices that are created in it, generate much of it in the rest of the car. However, as a counterpart to these vortices, the spoiler has to be more vertical thus presenting more air resistance and generating more dirty air. The spoiler of the AMR22 is simpler, creating a cleaner airflow behind it and it is, the floor and the diffuser of the car through the ground effect, responsible for generating the downforce that previously generated the vortices. Therefore, successive changes in regulations are effective.

6. References

- [1] Adrian Newey, chief technical officer and aerodynamicist of Red Bull Racing. How to build a car?". November, 2017.
- [2] Greg Stuart. "10 things you need to know about the all-new 2022 F1 car", F1 webpage. July, 2021. <https://www.formula1.com/en/latest/article.10-things-you-need-to-know-about-the-all-new-2022-f1-car.4OLg8DrXyzHzdoGrbqp6ye.html>
- [3] Simon McBeath. "Competition Car Aerodynamics". February, 2013. P73-158.

Memory Index

Chapter 1. Introduction.....	7
1.1 Project motivation	7
1.2 Change of the regulation	7
1.2.1 Increase in the number of overtakes.....	8
1.2.2 Wheel changes.....	9
1.2.3 Front wing and nose changes.....	10
1.2.4 Chassis (ground effect).....	11
1.2.5 Rear wing changes	12
1.2.6 Safety and sustainability.....	13
1.2.7 Financial regulations	14
1.3 Approximations and Peculiarities.....	14
Chapter 2. State of the art.....	17
2.1 History of aerodynamics in F1	17
2.1.1 1950 – 1959.....	17
2.1.2 1960 – 1969.....	18
2.1.3 1970 – 1979.....	19
2.1.4 1980 – 1989.....	21
2.1.5 1990 – 1999.....	22
2.1.6 2000 – 2009.....	23
2.1.7 2010 – 2019.....	24
2.2 Evolution of the front wing in F1	26
2.3 Front wing parts.....	30
2.3.1 Differences between 2016 and 2021 Front wings	33
2.4 Functions of the front wing	34
2.4.1 Modify the airflow path	35
2.4.2 Generate downforce	36
Chapter 3. Aerodynamic theory and CFD.....	37
3.1 Laminar And Turbulent Flow: the Reynolds Number.....	37
3.1.1 Boundary Layer.....	38
3.2 Navier Stokes Equations	39

3.2.1 Bernoulli Equation	40
3.3 Drag and Lift	41
3.3.1 Drag.....	42
3.3.2 Lift	44
3.4 CFD operation	47
3.5 Wind Tunnel Operation.....	48
Chapter 4. CFD Setup	50
4.1 Model selection	50
4.1.1 Differences between CADs and Real.....	51
4.2 Control Volume and Mesh	52
4.3 Convergency and Residuals	54
Chapter 5. Analysis of the results.....	55
5.1 Aerodynamic forces	55
5.2 Velocity And Pressure Distributions	58
5.3 c_p coefficient.....	62
5.4 Wake Structure and Vorticity.....	64
5.5 Reliability of the Results	68
Chapter 6. Environmental impact.....	69
Chapter 7. Economic analysis.....	71
Chapter 8. Conclusions and future works	73
Chapter 9. Bibliography	74
Annex I	78
Annex II	79

Figure Index

Figure 1: Control Volumes and Mesh	13
Figure 2: W07 (←) and AMR22 (→) Vorticity	14
Figure 3: Loss of downforce following a 2021 F1 car	8
Figure 4: Loss of downforce following a 2022 F1 car	9
Figure 5: Red Bull Wheel Changes	10
Figure 6: Mercedes Front Wing Changes 2021 vs 2022	11
Figure 7: Floor and Diffuser in 2022 car	12
Figure 8: Alpha Tauri Rear Wing Changes 2021 vs 2022	13
Figure 9: F1-75 Sidepods Air Flow Streamline	15
Figure 10: Williams FW44 Sidepod Hole	15
Figure 11: 1958 Cooper	17
Figure 12: Lotus 49B and the Beginning of the Ground Effect	19
Figure 13: Chaparral 2J	20
Figure 14: Lotus 78 and Colin Chapman's skirts	21
Figure 15: Minardi 197's Floor and Diffuser	22
Figure 16: Renault's Mass Damper	23
Figure 17: Mercedes Shark Fin	24
Figure 18: Drag Reduction System Mechanism	25
Figure 19: Fduct Mechanism	25
Figure 20: Halo	26
Figure 21: Evolution of the Endplate	27
Figure 22: March 711	27
Figure 23: Tyrrel 019 Front Wing	28
<i>Figure 24: MP4-23 Front wing</i>	<i>28</i>
Figure 25: McLaren Front wing 2018 vs 2021	29
Figure 26: Strakes in Front Wing	29
Figure 27: Front Wing Evolution	30
<i>Figure 28: Y-250 Vortex</i>	<i>31</i>

Figure 29: Front Wing Parts	33
Figure 30: Front Wings W07 vs W12	33
Figure 31: Laminar Flow vs Turbulent Flow	37
Figure 32: Boundary Layer Transition	38
Figure 33: Pipe with decreasing Area	40
Figure 34: Shear and Pressure stresses	42
Figure 35: Flow separation	43
Figure 36: Drag Force vs Streamlining of the Body	44
Figure 37: Airfoil Terminology	45
Figure 38: Mercedes Wind Tunnel.....	49
Figure 39: W07 CAD vs Real.....	50
Figure 40: AMR22 CAD vs Real	51
Figure 41: W07 Frontwing CAD vs Real.....	51
Figure 42: AMR22 Frontwing CAD vs Real.....	51
Figure 43: Control Volumes	53
Figure 44: AMR22 Frontwing Mesh.....	53
Figure 45: W07 Frontwing Mesh	54
Figure 46: Residuals and Convergency of the Simulations.....	54
Figure 47: Aerodynamic Efficiency vs Car Speed	58
Figure 48: W07 Frontwing Velocity Streamline	59
Figure 49: AMR22 Frontwing Velocity Streamline.....	59
Figure 50: W07 Frontwing Pressure Distribution	60
Figure 51: AMR22 Frontwing Pressure Distribution	61
Figure 52: F1 Front Wings' Cavities	61
Figure 53: Stagnation Point Solutions in F1.....	62
Figure 54: W07 Frontwing c_p coefficient	63
Figure 55: AMR22 Frontwing c_p coefficient.....	63
Figure 56: Wake of the Airflow for W07 Frontwing	64
Figure 57: Wake of the Airflow for AMR22 Frontwing.....	65
Figure 58: Flow Speed behind W07 Front Wing	65

Figure 59: Flow speed behind AMR22 Front Wing.....	66
Figure 60: Total Pressure Field behind W07 Front Wing	66
Figure 61: Total Pressure Field behind AMR22 Front Wing.....	67
Figure 62: Ferrari F1-75's Engine	78
Figure 63: Front View Front Wing Measurements	79
Figure 64: Top View Front Wing Measurements.....	79

Table Index

Table 1: Downforce and Air Resistance for 50 and 75 m/s	13
Table 2: Drag and Downforce for 25 and 50 m/s airflow	56
Table 3: Drag and Downforce for 75 and 100 m/s airflow	56
Table 4: Aerodynamic Efficiencies Comparison.....	57

Chapter 1. INTRODUCTION

1.1 PROJECT MOTIVATION

The purpose of studying the aerodynamics of the front wing of both Formula 1 cars is to get closer to the engineering of the fastest cars in the world and one of the most sophisticated engineering works worldwide where innovation and imagination are constantly needed instruments to achieve an aerodynamic and engine advantage.

As well, getting into the world of software simulation, especially in CFD (Computational Fluid Dynamics). This is a tool used by the different F1 teams, as well as by the FIA (Fédération Internationale de l'Automobile), the regulatory body of the competition, to reduce financial costs by the teams by avoiding using the wind tunnel, as to save time by being able to test more models in a faster way. In addition, the testing times in the F1 common wind tunnel are limited by the FIA, which is why it is very important to get the most out of it by using only the models that have given good results in the simulations with software.

1.2 CHANGE OF THE REGULATION

The FIA sought to do a great facelift in F1 in the year 2021, however, due to the global pandemic caused by the SARS-CoV-2 virus (COVID-19), the change of regulations was completed in the year 2022. This search for a makeover is since, in recent years, the aerodynamic improvements by the teams in terms of creating dirty air, turbulent air created by a car, which creates a reduction in the efficiency of the following car's aerodynamic surfaces, the number of overtaking has been seen drastically reduced. This has resulted in a clear reduction of followers due to the increase in the monotony of the sport (it should be noted that the launch of the docuseries "Drive to Survive" by Netflix, resulted in a rebound in the audience of Formula 1). In turn, the clear superiority of the Mercedes-AMG

PETRONAS F1 team since the last major rule change, which was ushered in at the beginning of the hybrid era, has also affected the audience of this competition. It is also important to note that the changes in regulations, in terms of the structure of the car, are completely aerodynamic, and the power unit of 2021 will be used, Annex I shows a datasheet of the Ferrari F1-75 engine, which is made up of the power-unit (gasoline engine) and the ERS system (electric engine), which is speculated that it could be the most powerful during the 2022 season. It is for these reasons that the FIA tries to renew the image of this sport by changing the following key aerodynamic aspects:

1.2.1 INCREASE IN THE NUMBER OF OVERTAKES

This is the main goal of the change in the regulations, thanks to a drastic reduction in dirty air from cars, they will be able to chase each other more continuously without losing downforce as drastically as before. The different simulations have shown that the F1 cars of 2021 suffered a downforce reduction of 35% when they were 20 meters from the leading car and 47% at a distance of 10 meters, increasing the understeer of the car and therefore, making it more difficult to drive. In contrast, the F1 cars of 2022 would only suffer a downforce reduction of 4% at 20 meters and 18% at 10 meters as can be seen in Figure 3 and in Figure 4. This change will help increase the number of overtaking.

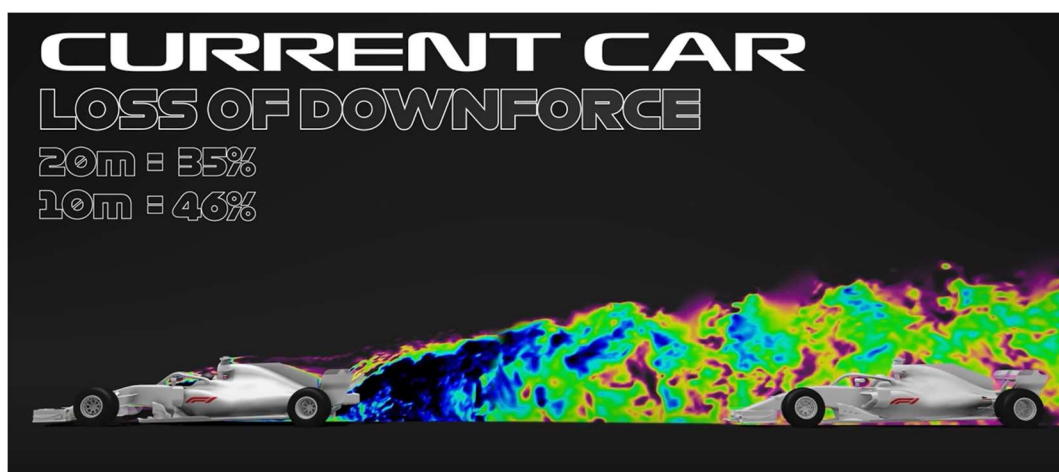


Figure 3: Loss of downforce following a 2021 F1 car



Figure 4: Loss of downforce following a 2022 F1 car

1.2.2 WHEEL CHANGES

Regarding the wheels and tires, the changes are severe. First, the wheel size increases to 18 inches, this results in a reduction in the overheating of the tire when it slides thanks to adding new compounds materials and the decrease in size. Secondly, new low-profile tires are incorporated, which aim to reduce the deformation of the sidewalls of the tires and consequently, a reduction of the wake effect produced by them.

Two other important features added around the wheels are the inclusion of over-wheel winglets and wheel covers. Although the launch of airflow directly towards the tires translates into an increase in the car's downforce, it is also one of the great causes of the dirty air that is created, which is why the inclusion of a wheel cover was necessary to reduce turbulence created in the wake of the car. The function of the over-wheel winglets is to help control the wake coming from the front wheels and away from the rear wing, also reducing dirty air and allowing close racing. The changes explained above are shown in Figure 5.



Figure 5: Red Bull Wheel Changes

1.2.3 FRONT WING AND NOSE CHANGES

The 2022 regulation change brings with it a new, more simplified form of the front wing, which had already been simplified in previous years. Its function is to generate a constant downforce when running close to another car and, in turn, to generate the minimum possible wake so that if it is being chased by another car, it generates the minimum amount of dirty air.

Thanks to reducing the number of elements and eliminating the connection between the flaps and the main plane and by reducing the winglets and sharp edges, the force of the vortices generated in the front wing is substantially reduced, reducing dirty air. Therefore, it is not necessary to direct the dirty air away from the car and this dirty air is controlled by the wheel covers as had been mentioned before. In addition, this spoiler loses less downforce when receiving dirty air, since being flatter surfaces its ability to work with turbulent air is greater.

In short, the ability of this piece to generate downforce on its own remains relatively constant. On the other hand, due to the elimination of different parts such as the strakes and the footplate, as well as the vortex generators, the downforce capacity generated by the rest of the car is lost thanks to the air redirected by the front wing. In turn, it is these

simplifications that drastically simplify airflow, reducing the amount of dirty air generated by the F1. It is for this reason that the ground effect comes to play a crucial role in the aerodynamics of the vehicle. The variation between the front wings of the Mercedes team between the year 2021 (figure above) and the year 2022 (figure below) is shown in Figure 6.



Figure 6: Mercedes Front Wing Changes 2021 vs 2022

1.2.4 CHASSIS (GROUND EFFECT)

Due to the clear simplification of the ailerons, they were going to see their ability to generate reduced downforce, that is why it is necessary to emphasize the ground effect to recover downforce and, in turn, reduce dirty air from the wings. ailerons. The barge boards of today's cars are designed to send vortices under the floor of the car to increase the downforce, on the other hand, this downforce is greatly reduced when the distance between cars is smaller.

The design of the 2022 cars uses the pressure difference between the car and the road; by increasing the speed of the fluid, the pressure exerted by the fluid on both surfaces decreases, conserving energy, leading to depression or downforce. In these new cars, the large majority of the aerodynamic charge produced by the car comes from the ground effect.

It should be noted that the simplification of the car's floor, as well as its sides, puts an end to bargeboards, curved and vertical plates located on the side of the car, between the tires and

the pontoons. These serve to generate an aerodynamic benefit by redirecting airflow, generating vortices that sealed the old flat bottom, expelling turbulence generated by the front tires, and decreasing the speed of entry of airflow into the rear sidepod. Below, in Figure 7, the new floor is shown next to the diffuser of the 2022 F1.

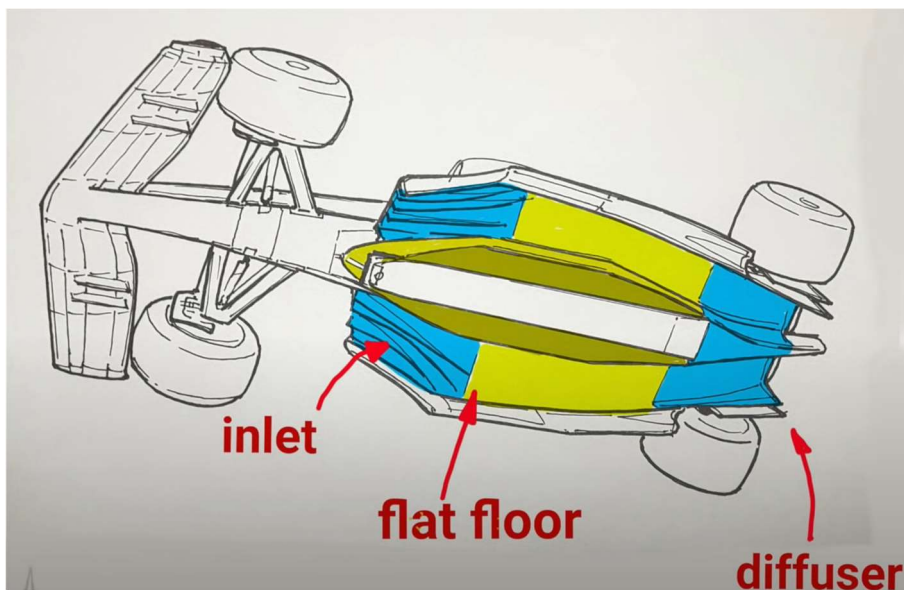


Figure 7: Floor and Diffuser in 2022 car

1.2.5 REAR WING CHANGES

The drastic change in the rear wing is reflected in a variation in the shape of the rear wing. While the 2021 spoiler was a square spoiler with two similar wing elements along the entire length and an endplate for both the beginning and the end of the structure that is typically square. The function of these endplates is to force the airflow to follow the contour of the wing and not escape through the sides, thus increasing the downforce created by the aileron.

The 2022 spoiler eliminates these end-plates by allowing air to escape through the sides and drastically reducing the amount of dirty air produced by the car by eliminating the vortices created at the junction between the end-plate and the flap, but as a result, there is also a clear decrease in the downforce produced by the spoiler, which is why it is necessary to resort to the ground effect to maintain the same level of downforce.

The curve of the rear wing of the new wing forces the dirty air into the diffuser area as the airflow from the ground effect pushes all that dirty air over the chasing car. This effect is produced thanks to the new low wing element of the aileron, which creates a zone of low pressure just above the diffuser and increases the ground effect. The variation between the rear wings of the Alpha Tauri team between the year 2021 (figure above) and the year 2022 (figure below) is shown in Figure 8.



Figure 8: Alpha Tauri Rear Wing Changes 2021 vs 2022

It is important to highlight the increased power of the DRS during this season, the operation of which is explained in [2] 2.1.7. This is because the upper flap of the rear wing, the one in which the DRS is involved, has a larger area, and therefore when the system is activated, the percentage of drag that is reduced is greater than in other seasons.

1.2.6 SAFETY AND SUSTAINABILITY

The safety of these cars has been improved thanks to an increase in energy absorption of 48% and 15% of the front and rear parts of the car, respectively. In turn, learning from past lessons such as the Romain Grosjean accident at the 2020 Bahrain Grand Prix, in the event of an accident the fuel tank will never be exposed by separating the power unit in the event of an accident. However, these improvements have led to an increase in the car's weight of

5%, from 752kg to 790kg, which translates, in that we find ourselves with the heaviest F1 in the modern era of competition.

In turn, in a 5% increase in the percentage of biofuel used by automobiles, with a total of 10% sustainable ethanol. This change will promote F1's image of sustainability as well as bring it closer to the 2025 goals of using a 100% sustainable fuel, which will be made public for use by the general public, and 2030 of having zero carbon net emissions.

1.2.7 FINANCIAL REGULATIONS

The 2022 season will be the first to include a cost cap. The total cost with the performance of the car is capped at \$ 175 million. Since large teams with a much higher salary capacity than the rest will see their monetary superiority in terms of car performance costs diminished, in this way equality in the championship will increase substantially.

In addition, the fact that the cars are more equal ensures overtaking in which the driver's ability to overtake is accentuated concerning the previous one, downplaying the top speed gained with the DRS (Drag Reduction System) and overtaking in which absolute superiority reigns between cars.

1.3 APPROXIMATIONS AND PECULIARITIES

Next, a dissertation will be carried out on the greatest advances and most disruptive approaches by the different teams in the face of this change in regulations, as well as the main problems they face.

The introduction of gills by some teams, such as Aston Martin or Ferrari, on the sides of the car that seek to cool the power unit, in addition, this air is redirected back towards the lower part of the rear wing, called the beam wing, or in the case of Aston Martin, to the floor of the car to thus achieving increased aerodynamic efficiency by creating more downforce. In particular, the Ferrari team has tried to maximize this downforce by including very

aggressive sidepods which are also capable of redirecting the airflow to the rear beam wing. In Figure 9, you can see the airflow streamlining through the pontoons of the F1-75.



Figure 9: F1-75 Sidepods Air Flow Streamline

Despite the great differences in the sidepods of the cars, one of the most striking next to the Ferrari is the Williams, it has a hole in the middle of the sidepod which can be seen in Figure 10, whose function is to provide a neat airflow to the rear of the sidepod and the floor. This has been possible thanks to the fact that the valid presents the SIS (side impact spar) placed in the rear part of the inlet entry position. In addition, the single-seater has much more discreet sidepods than the rest of the cars, very similar to those presented by the Mercedes team after the drastic change that the W13 underwent after the Bahrain tests.

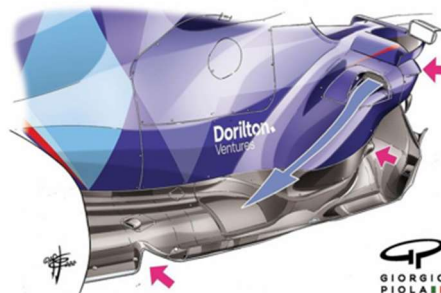


Figure 10: Williams FW44 Sidepod Hole

One of the main problems that the teams are having to face is the so-called porpoising, an old problem from the 80s, which with the return of the ground effect, has reappeared. This occurs because the cars are not capable of offering a constant downforce, the floor of the car ends up touching the ground, and just at that moment, all the aerodynamic load is lost, repeating the process over and over again. This results in cars that are more difficult to drive due to the driver's lack of confidence in braking the car due to lack of downforce and constant bouncing of the car off the ground. This problem could be solved by: including harder damping, increasing the height of the car, or including the mass damper explained in [3] 2.1.6. However, neither team wants to include any of these solutions as it would compromise the efficiency of the rest of the car.

Chapter 2. STATE OF THE ART

2.1 HISTORY OF AERODYNAMICS IN F1

2.1.1 1950 – 1959

At the start of the competition in 1950, F1 cars focused their speed purely on engine power, with aerodynamics playing a minor role in car design. The same founder of Scuderia Ferrari, Enzo Ferrari expressed this situation in the following sentence: "Aerodynamics is for losers who don't know how to make engines."

It would be in these early years when Juan Manuel Fangio, with an elegant and aggressive driving style, would dominate the competition, winning 5 drivers' championships. At the beginning of the decade, these vehicles had the engine placed in the front, the airflow did not detach from its surface until it reached the pilot's seat. The change to the rear engine came from the hand of a Cooper in 1958 shown in Figure 11, this provided an increase in the safety of the vehicle in case of impact, obtaining a physically smaller powertrain by not needing the use of a transmission shaft.



Figure 11: 1958 Cooper

These early cars had a bullet or drop shape, the most aerodynamic shape. This helped the flow through the vehicle to be quite laminar and besides, an attempt was made to minimize

the frontal area. On the other hand, these cars were extremely dangerous and difficult to drive because this way, very efficiently reduced drag, but at the same time, the downforce necessary to control the power of these cars was not considered. This is shown in the words of Tony Brooks, Formula 1 driver from 1956 to 1961: "In the early years the first rival was the circuit, if the car skidded you were out". This is why during these years, in addition to the fact that the energy absorption capacity of cars in the event of an accident was much lower than today, cars were also more difficult to drive, and this resulted in a large number of accidents, resulting many of these mortals.

2.1.2 1960 – 1969

It wasn't until the late 1960s that aerodynamics began to take on a bigger role. The discovery of the ground effect and the progress in the study of aerodynamic profiles were events that would mark the design of cars in the coming years, the cars began to be wedge-shaped, thus improving their aerodynamics. The first team to implement the ground effect was Lotus, which with its Lotus 49B designed by Colin Chapman shown in Figure 12, was able to take advantage of the negative lift forces generated by the pressure difference between road and vehicle to increase the grip of the tires when passing through a curve at high speeds. It was on this same car that the primitive front wing appeared for the first time in the form of small, raised spoilers on the nose of the car. This car was very promising, but at the same time very fragile since it was not known how to manage the airflow effectively. This was not a good thing, as during the first few years the cars were faced with major reliability problems. Different teams copied this technique by placing ailerons in different parts of the vehicle, a typical place was in the suspensions, producing various mechanical breaks. As well, the first rear wing appeared in this car as a curved sheet of metal.



Figure 12: Lotus 49B and the Beginning of the Ground Effect

Trying to mitigate the problems of dirty air coming from the other cars, Colin Chapman decided to raise the rear wing. This involved a much messier and more turbulent airflow, and the vortices generated began to play a crucial role in the aerodynamics of the car.

However, the increase in the height of the rear wing came hand in hand with a drastic increase in the number of accidents, and therefore the rear wings were banned. Instead, the teams added new models of rear spoilers, small ailerons much smaller and close to the surface of the car.

Later, the rear wings were reintroduced with their respective regulations which limited the height, dimensions, and methods of attachment to the rest of the vehicle.

2.1.3 1970 – 1979

It was this time, one of the most entertaining in the sport, various family and small teams would join it, standing up to those with larger budgets. However, during a long period of F1, from the late 1960s to the early 1980s, not all the teams had cottoned to the benefits of the ground effect. One of the big problems with this ground effect is understeer in the event of encountering an irregularity in the circuit by losing all downforce instantly. This understeer ends up resulting in a departure from the circuit with its consequent accident. This was an era in which crazy ideas appeared in the competition, some of them did not work and ended up being an anecdote in the history of the sport, such as the Tyrrel P34 from 1976, the only one with 6 tires, the March 721 from 1972, with an oval spoiler; the Benetton Tyrrel 012 from 1983, with a wedge-shaped spoiler and a long etcetera. In turn, this date also led to

innovative designs that would remain in the future of these cars, such as the appearance of slick tires by Firestone in 1971, which allowed a greater amount of tire in contact with the asphalt, and therefore, greater adherence to it; the ground effect used by the Lotus 78 which we will discuss in more depth below; the vacuum effect of the Brabham BT46 from 1978, based on the iconic Chaparral 2J shown in Figure 13, designed by Gordon Murray, by including a fan at the end of the car, this stuck to the circuit increasing its downforce; the inclusion of the carbon fiber chassis of the 1981 McLaren, which lasts to this day, through the different arrangement of the fibers of the material made the monocoque stiffer in one direction and more flexible in another. All these inventions would mark an era marked by change and innovation in competition such as the 70s.



Figure 13: Chaparral 2J

The Lotus 78 shown in Figure 14, designed by Colin Chapman, was an advance that, until prohibited by the regulations, was used in F1. The use of the ground effect through the inclusion of some inverted wing-shaped side pontoons gave the car a greater grip and a large increase in speed when cornering, achieving forces of approximately 3g, that is, the car appeared to weigh 3 times its weight, but without increasing the drag suffered. The single-seaters of the late 70s stood out for mounting large wings and rear tires.



Figure 14: Lotus 78 and Colin Chapman's skirts

2.1.4 1980 – 1989

It was in the late 1970s and early 1980s that the era of turbocharged engines began, the inclusion of the turbo allowing the weight and size of the engine to be reduced. The overfeeding of the engine with a subsequent increase in its pressure and, therefore, greater power offered to the vehicle. On the other hand, due to the disproportionate increase in engine power, which sometimes exceeded 1400 hp, and the lack of safety of the cars, the FIA in 1989 would end up prohibiting the turbo by prohibiting the supercharging of the engines.

The increase in speed when cornering and the increase in power of the engines resulted in a drastic increase in the number of accidents, and this, as always in F1 history, was followed by a change in regulations. Therefore, in 1981 the use of side skirts was prohibited and in 1983 the obligation to use a flat bottom was established, ending the period of greatest development in the car floor. This meant the end of the ground effect, which would not play an important role in F1 again until the arrival of the cars of 2022.

The need to introduce air at high speed in the lower part of the car led to some designs in which the front wings were removed to avoid obstructing the entry of airflow to the underside of the vehicle. The ailerons saw their sizes reduced and the cars narrowed again.

It should be noted the appearance of an important innovation such as the invention of the active suspension which helped the aerodynamic components to be in an optimal arrangement for their operation, in addition to allowing independent control of each wheel,

thus increasing the grip and therefore the safety of the vehicle. The active suspension works by using an oil pump attached to the engine to generate hydraulic pressure. The hydraulic pressure is used to extend or shorten actuators at each wheel depending on what they need to do to achieve the desired ride height.

It was also at the end of this decade that the effects of exhaust gases with the blown diffuser, shown in Figure 15, began to be investigated, reaching its maximum expression with the Brawn BGP 001, with the addition of a double diffuser, in 2009 gave the world championship to Jenson Button. Increasing the downforce at the rear of the car.

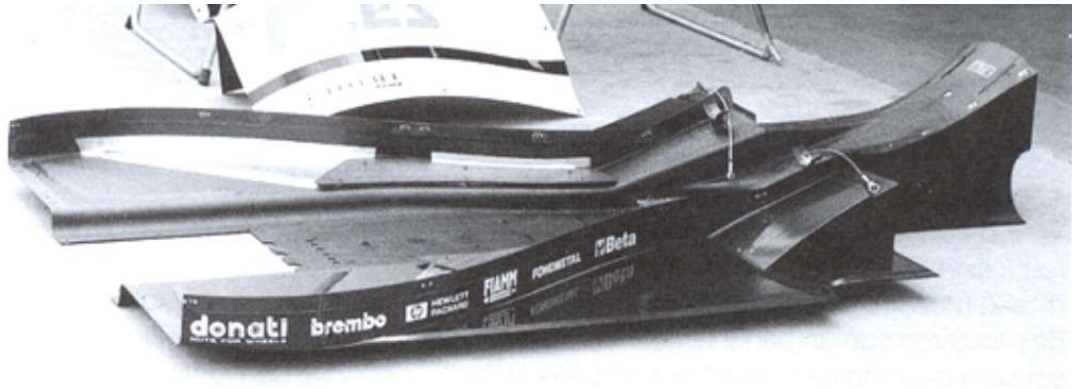


Figure 15: Minardi 197's Floor and Diffuser

2.1.5 1990 – 1999

The beginning of this decade would witness one of the greatest rivalries between drivers in the history of F1, Ayrton Senna against Alain Prost, 3- and 4-times drivers' world champions respectively. Sadly, this would come to an end with the fatal accident of Ayrton Senna at the Imola GP in 1994. As a result of this mediatic accident, and many others, the FIA was forced to carry out a change in regulations that would increase the safety of the cars. Some of these changes were, the return to the grooved wheels, to reduce the speed of the car; drilling holes in the air intakes to reduce the "air ram" effect, and reducing power. In addition, a wooden board was included on the floor of the car to check that the cars maintained the minimum height, which is maintained to this day and is responsible for the sparks that F1 cars emit

when reaching high speeds. Later, the opening of the cabin was increased, and the size of ailerons and other aerodynamic elements was reduced, as well as the size of the chassis.

2.1.6 2000 – 2009

The beginning of the millennium brought with it the monopolization of the championship by Michael Schumacher's Ferrari until 2004. This superiority was due to two factors, a driver with above-average skills, and the best car on the grid. The improvements in terms of cooling, reduction of the size of the side-pods, the change of the angled front wing to a conventional flat wing, and larger bargeboards, together with great reliability made the Ferrari F1-2000 the winner, for the next few years. The different cars of the Maranello Scuderia would be a development of the Ferrari F1-2000.

It would not be until 2005, that the Renault of Fernando Alonso, snatched the hegemony from Schumacher. A regulation change was carried out in which the aim was to keep the distance between the front wing and the asphalt constant, which increased the vibrations of the car.

In response to this, the Renault team introduced the mass damper, a free weight of about 10 kilograms suspended between two springs inside a cylinder, this was placed in the nose of the vehicle. This mass damper, shown in Figure 16, worked as a shock absorber capable of absorbing the strong vibrations produced by the irregularities of the asphalt, which, after its ban, would make it clear that it was a great advantage over other cars.

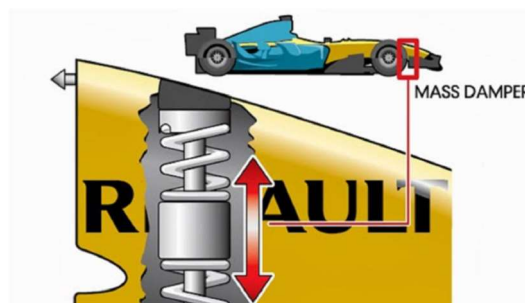


Figure 16: Renault's Mass Damper

In this decade it is worth highlighting the appearance of the shark fin in F1 cars shown in Figure 17, this is an added barrier behind the rear air intake that serves as a barrier so that air cannot cross from one side of the car to the other. In this way, the airflow that reaches the rear wing is aligned and laminated, increasing its effectiveness. The effect of this is especially remarkable in curves, when entering a curve at high speed the car tends to go out of the curve due to the centrifugal force, instead the wing exerts an opposite lateral force that maximizes grip, helping to counteract the drift of the car.

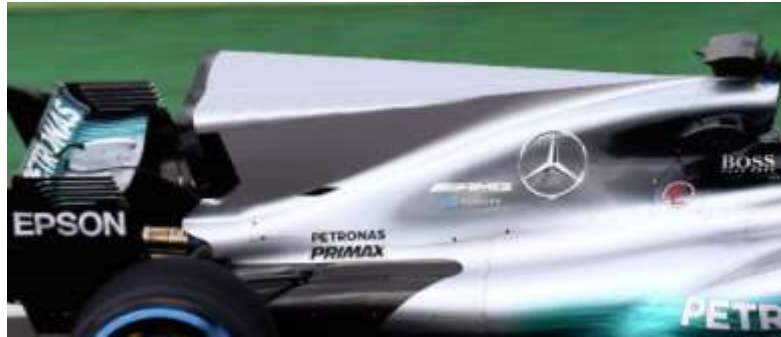


Figure 17: Mercedes Shark Fin

The appearance of the KERS (Kinetic Energy Recovery System) and its use brought many headaches to the different teams. This is a system based on the storage of the thermal energy released by the car in battery braking, for its later use in overtaking, thus achieving an extra speed. However, this system turned out to be very expensive and not very effective due to the extra weight that is added to the car. This is why it ended up being replaced by the MGU, an energy recovery system connected to the engine turbocharger.

2.1.7 2010 – 2019

At the beginning of the new decade, in 2010, McLaren implemented an F-duct in their cars, whose opening was on the nose, which the pilot activated to change the turbulence of the air on the rear wing and achieve a lower downforce and, consequently, increase speed on the straights.

In 2011, the mobile rear wing, commonly known as DRS shown in Figure 18, would come to F1, this is activated manually by the pilot. It consists of a mobile flap that is positioned

flat when an increase in the vehicle's top speed is required on a straight line and is positioned flat when a greater downforce is required when going through a curve.

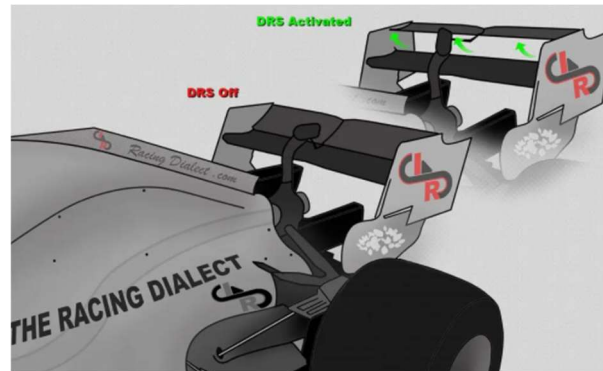


Figure 18: Drag Reduction System Mechanism

After the incorporation of the DRS, came to an improvement of the F-duct which mechanism is shown in Figure 19, which would be renamed the S-duct in the Mercedes W06 car. This works by opening a hole in the inside of the rear wing, which is covered while the DRS is inactive. When it is opened, the incoming air is expelled over the rear diffuser, and this, in turn, expels it over the ground from the car floor to the front wing, significantly reducing downforce and thus increasing top speed.

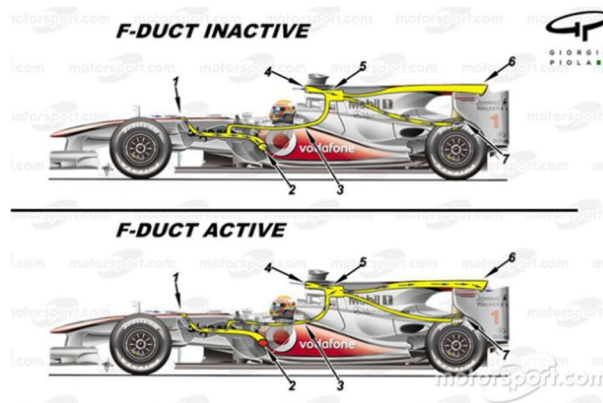


Figure 19: Fduct Mechanism

One of the great additions of the decade in 2018 was the halo, shown in Figure 20. A safety system that protects the cockpit from impacts from external objects, consists of three flexible titanium bars located in front of and above the driver's head, which weighs 10 kg. Finally,

the system, which at first did not end up being liked by the scuderias, nor by pilots, nor by fans, would end up being acclaimed by all, by demonstrating its effectiveness in different accidents such as that of Romain Grosjean at the 2020 Bahrain Grand Prix. in which the halo saved his life by protecting his head from a hit against the guardrail, or Lewis Hamilton with Max Verstappen in the 2021 Italian Grand Prix, in which the halo prevented the RedBull car wheel from impacting on the head of the English.



Figure 20: Halo

2.2 EVOLUTION OF THE FRONT WING IN F1

Initially, F1 cars did not have a front wing and were drop-shaped, to minimize drag without considering downforce. It wouldn't be until the Lotus 49B in 1967 that we wouldn't see the first front wing. A very simple wing, which had only two flaps on each side of the nose, the front wing was born and its evolution and increase in complexity would not cease until 2022.

It was not until 1970 that most teams introduced endplates at the end of each flap with the function of preventing the flow of air between both sides. This was a significant advance, and over the years the size of these endplates has increased considerably. The evolution of this piece is shown in Figure 21.



Figure 21: Evolution of the Endplate

In addition, during this decade curious designs were observed such as that of the March 711 shown in Figure 22, which, with a raised front spoiler concerning the rest of the car and with an oval shape, tried to maximize its aerodynamic efficiency. Instead, the results fell short of expectations, and the team would revert to a more conventional layout during the following season.



Figure 22: March 711

Instead, it would not be until 1984, that all the teams incorporated the front wing on their car. This was because, at that time, the effects of adding this part were not fully understood, and various tests such as the March 711 brought with them many problems in the reliability of the car. In addition, in this same year, the two-flap spoiler appeared for the first time.

It was in 1990 when the Tyrrell 019, whose front wing is shown in Figure 23, featured a raised nose to increase the airflow under the car for increased downforce. It also featured two vertical fins that sought to channel the airflow around the wheels.



Figure 23: Tyrrel 019 Front Wing

It was in 2001 when the arrival of the curved flaps by the Ferrari F2001 would revolutionize the aerodynamics of the front wing, this car showed clear superiority over the rest of the grid since it allowed to redirect the airflow more easily and obtain high aerodynamic efficiency. In terms of engine, the Williams of this same year with a BMW engine showed more power. Finally, Ferrari would win its third consecutive title.

The extreme in terms of the curvature in the wings can be found in the Vodafone McLaren Mercedes MP4-23 in 2008, whose front wing is shown in *Figure 24*, with which Lewis Hamilton would win his first drivers' world championship. In this, in addition to the raised flap, we can see how the complexity of the part increases drastically, dividing the aileron into 3 lower flaps and one upper flap, in addition to the arrival of the footplates or dancefloors, the flat surfaces at the end of each endplate.



Figure 24: MP4-23 Front wing

The complexity of this piece would increase exponentially during the following decade thanks to advances in technology developed with the wind tunnel and CFD. A greater number of flaps and vortex creators would be added until reaching the 2018 wing. It was from here that the FIA tried to start simplifying the part through regulation. He eliminated the vertical flaps whose function was to expel the airflow to the outside of the vehicle and

limited the total number of flaps to 5. Due to these restrictions, the shape of the spoiler changed since an attempt was made to seek the expulsion of air outwards of the vehicle through the shape of the flaps, rather than with the vertical flaps, which had been banned. A comparison between McLaren's front wings for the years 2018 (left) and 2021 (right) is shown in Figure 25.



Figure 25: McLaren Front wing 2018 vs 2021

In recent years the so-called fences or strakes, shown in Figure 26, have also appeared, these are sheets that are found in the lower part of the spoiler and whose function is to reinforce the Y-250 vortex and weaken the turbulence created by the tires. On the other hand, with the 2022 regulation change, these fences will no longer appear on the wing since they are not as necessary as before thanks to the inclusion of wheel coverage and wheel winglets.



Figure 26: Strakes in Front Wing

As can be seen in Figure 27, the complexity of this piece has increased over the years, until 2018. Below is a comparison of the Formula 1 wings over the years, to observe their evolution.



Figure 27: Front Wing Evolution

2.3 FRONT WING PARTS

The front wing is made up of many parts with different functions, this has been divided over time into more parts for this, in addition to being able to continue to achieve high downforce requirements and efficient airflow redirection, alleviating problems of bending that the aileron would suffer in the case of being a single piece.

This is why in recent years the controversial concept of Flexi-wing has been established. The regulation states that all aerodynamic parts must be completely rigid, except for the DRS. During the last competitions, some teams have shown their complaints, claiming that the wings of other teams were flexing too much, which would be giving them a small aerodynamic advantage.

Also, unlike the rear wing, whose design is usually quite restricted due to regulations; the front wing usually shows severe changes from one season to the next. However, in this new

regulation change, 2021-2022, both the front and rear wings will experience drastic variations.

The different parts of a front wing are as follows:

- The main plane is the base of the spoiler and is its main element. It is the largest piece of the spoiler, and it is intended to be as close as possible to the asphalt, within the limits of the regulations and the conditions of each circuit. Its inverted wing section tries to generate the most downforce. It has two parts: a control section, the central section of the piece, which is standardized by regulations and is common to all teams; and the rest of the piece, in which the teams, within the allowed dimensions, design the piece based on the desired characteristics.

- A series of winglets, or winglets cascade, and flaps, which are located on the main plane. Their design was not very limited and that is why, in this area of the spoiler, we used to see great differences between the teams. They seek to generate downforce and divert the flow of air, thus avoiding collision with the tires. In addition, in their union in the main plane, these generate the most important vortex of the F1, the Y250, shown in

Figure 28. It is produced due to the union of the air coming from the high-pressure zone and the low-pressure zone of the flaps. This vortex is so named since it passes 250 mm from the central area of the aileron. However, in the new 2022 cars, this vortex disappears by increasing the simplicity of the flaps joining directly at the nose of the spoiler. Its complexity has been increasing drastically over the years, and the new regulation change seeks to simplify substances thereof.



Figure 28: Y-250 Vortex

- An endplate is the piece that is located at the two ends of the aileron. It is also found on the rear spoiler and the winglet. They are vertical pieces whose function is not to allow a union between the low-pressure and high-pressure areas of the aileron. Thanks to this, they increase downforce and reduce drag; Also, thanks to their curvature, they are capable of directing the vortices that are generated in their joints towards the outside of the car.
- A footplate, is placed at the bottom of the endplate. Thanks to its curvature, it is capable of generating vortices that improve the behavior of the airflow next to the wheels. Looking for it to behave like a covered tire, which brings with it a significant aerodynamic improvement.
- The nose of the spoiler joins the front wing with the rest of the car. It is a safety structure, it is hollow at the tip, and thanks to its ability to absorb impacts, it prevents the energy of the accident from reaching the pilot in the event of a crash. In turn, it presents spaces between the neutral zone of the main plane and the tip of the same to increase the aerodynamic efficiency of the car.
- Some fences are located in the lower area of the spoiler. Its function is the redirection of the airflow and the transformation of the turbulent flow into a laminar one. These are also capable of creating vortices, which improve the performance of the car.
- Curved vane, which were not found in the 2021 or 2022 ailerons but were found in one of the ailerons that is the object of study in 2016, are vertical flaps found on the sides of the flaps whose function is to evacuate air to the outer area of the spoiler so that it avoids the tire.

The different parts of the front spoiler mentioned above are shown in Figure 29.

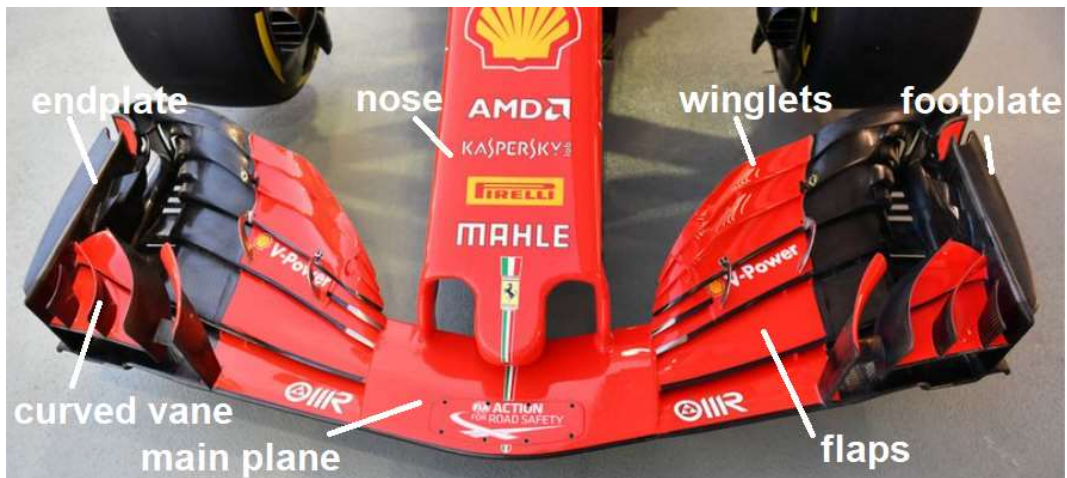


Figure 29: Front Wing Parts

2.3.1 DIFFERENCES BETWEEN 2016 AND 2021 FRONT WINGS

Considering that one of the spoilers analyzed in the study is from the year 2016, from the Mercedes W07, a brief dissertation will be carried out about the differences between the spoilers of this year and those of the year 2021. In Figure 30 you can observe the spoiler of the W07 of the year 2016 (up) and that of the W12 of the year 2021 (down).



Figure 30: Front Wings W07 vs W12

The main difference that can be observed between both wings is the elimination of the vertical flaps, which had the function of expelling a certain part of the airflow out of the vehicle. Also, the end of the extreme curvature after these vertical flaps.

As it can be seen in the 2021 wing, the nose is reduced in size, these vertical flaps and the extravagant curvature of the flaps after them are gone, which results in a change in the shape of the wing. The upper flap takes a much more horizontal shape, being seen in some spoilers as this spoiler even has an inverted U shape. This seeks to be the horizontal flaps themselves due to their shape, and replacing the function of the vertical ones, the ones in charge of expelling the air towards the outside of the vehicle.

2.4 FUNCTIONS OF THE FRONT WING

This is the first element of the car that comes into contact with the air. The functions of the F1 front wing are diverse, being considered the most important aerodynamic part in the cars of 2021. Thanks to its high complexity, the teams can modify the path followed by the airflow through the car, diverting or driving it through vortices, and in turn, increase the downforce generated by the part, while minimizing the drag.

The cost of this piece is high, between about 170,000 and about 225,000 dollars. The price of the material used is priced at about \$ 22,000.

To this expense must be added CFD testing, and later, in the wind tunnel, for which it is necessary to create a scale model and pay a team of approximately 50 engineers a salary that is usually normalized at 2,200 dollars a day per engineer.

Furthermore, the configuration of the front wing is often intrinsic to the nature of the circuit. If we find ourselves on a high downforce circuit with a lower average speed, such as Monaco, for example, the front wing will be more robust to play a more important role; On the other hand, in races where long straights and top speed reign, such as Monza, the front wing will be reduced in size.

2.4.1 MODIFY THE AIRFLOW PATH

The main objective of the front wing is the modification of the airflow for its subsequent interaction with the rest of the vehicle in an optimal way. The wing generates downforce not only by itself, but the flow redirected by it is responsible for approximately 40% of the total downforce.

In turn, this piece is also capable of converting the airflow from turbulent to laminar. That is, to order it if two cars are very close together, trying to reduce the effects of dirty air as much as possible.

2.4.1.1 Avoid tires

Preventing the air from hitting the wheels directly is essential, this would generate great resistance or drag, as well as greatly disrupt the airflow, consequently reducing the efficiency of the car.

This is done through a set of flaps positioned in front of the tires. These take care of moving the airflow away from the wheels and suspension, pushing it upwards.

2.4.1.2 Generate vortices

The main reason for the high complexity of this piece is its importance in the generation of vortices. The vortices are used to modify the state of the boundary layer of the air that surrounds the surface of the car. These are created by small pieces that break the laminar state of the air, inducing a rotational movement in the air, thus achieving greater energy. Vortices are created in the spoiler that has different effects: sealing vortices and those that reduce tire drag.

What these vortices, those created in the first flaps, can also seek is to prevent the detachment of the boundary layer from occurring, by increasing the energy of the air and thus increasing the aerodynamic load generated.

The sealing vortices are highly intense vortices that, as they travel the car towards its rear, rotate with great intensity, preventing the entry of more air to the flat bottom and maintaining

the low-pressure area under the car. These act in a similar way to the sliding skirts that were incorporated into single-seaters to create the ground effect.

The vortices that reduce tire drag seek redirection of airflow before it meets the front tires. This is done by expelling the flow towards the external area of the vehicle or by guiding it between the elements of the suspension.

2.4.2 GENERATE DOWNFORCE

Generating downforce, while minimizing drag, is one of the key functions of the front wing, although it is not its main objective. This is carried out by reducing the distance between the main plane and the asphalt to the minimum allowed by the regulations, in such a way that the air accelerates in this free space and a great depression is created under it.

Chapter 3. AERODYNAMIC THEORY AND CFD

Before carrying out the aerodynamic study, it is necessary to know the physical properties and laws of fluids, their equations, and their behavior. In this way, we will understand the mathematical models extracted from fluid mechanics on which CFD is based.

3.1 LAMINAR AND TURBULENT FLOW: THE REYNOLDS NUMBER

A fluid flow has two different regimes: laminar and turbulent. These behave in very different ways from each other.

Laminar flow shows a minimum amount of mixing between the layers. It is a very smooth and even flow. As the speed of the fluid increases, the mixing between the layers becomes more evident, entering the transition zone between the laminar and turbulent flow. From a certain speed, the turbulent regime is reached, which is characterized by a chaotic movement of the fluid. The figure shows the differences between laminar flow and turbulent flow. Figure 31 shows the differences between laminar flow and turbulent flow.

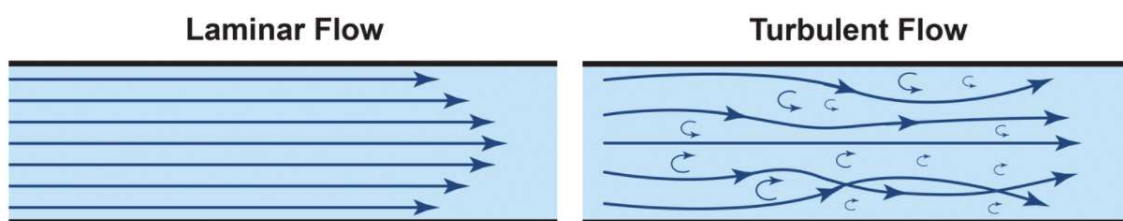


Figure 31: Laminar Flow vs Turbulent Flow

Because laminar flow is much smoother and there is less mixing between the layers, it is much easier to model than turbulent flow.

To know what regime we are in, the so-called Reynolds number is used. Osborne Reynolds carried out a series of measurements to find out which were the factors that influenced the flow regime, thus obtaining the dimensionless Reynolds number:

$$E\ 3-1 \quad Re = \frac{\rho * v * L}{\mu}$$

Where ρ represents the density of the fluid, v its velocity, L is the characteristic distance, and depends on the geometry of the body being treated, and μ is dynamic viscosity.

The Reynolds number shows us the ratio of the forces of inertia, those related to the moment of the fluid and therefore those responsible for its movement, between the viscous forces or she, which are the friction forces, these slow down the fluid due to its viscosity.

If viscous forces dominate, the flow will be laminar, and the fluid particles will have a straight trajectory; a low Reynolds is obtained. If inertial forces dominate, the flow will be turbulent, and a high Reynolds is obtained.

3.1.1 BOUNDARY LAYER

The boundary layer is that region of the fluid whose movement or dynamics is influenced or disturbed by an interaction with a solid, shown in Figure 32. The region between the contact zone with the solid and the zone in which the fluid reaches 99% of the velocity of the undisturbed fluid is considered.



Figure 32: Boundary Layer Transition

Like any other zone in the fluid, the boundary layer can present a laminar regime, as well as a turbulent one, as a transition between the two. If, as the fluid comes into contact with the solid, the velocity gradient in the area of contact with the solid becomes opposite to that of the fluid, what is known as boundary layer detachment or flow separation. This is very detrimental in some cases as the fluid separates from the fluid surface, failing to create an aerodynamic load and that is where the vortex generators appear, increasing the energy of the flow and sticking it to the surface of the front wing.

3.2 NAVIER STOKES EQUATIONS

The Navier-Stokes equations are a set of equations that can describe the behavior of any Newtonian fluid, those whose viscosity can be considered constant when there are not big temperature gradients. A set of non-linear partial differential equations, of which a generic solution has not yet been obtained. These are the main tool of CFD analysis.

These equations arise from the application of conservation of mass, conservation of energy, and conservation of momentum to a control volume. From these conservations, we obtain the following equations as a function of time: an equation of continuity, three equations of conservation of momentum, one for each dimension, and an equation of conservation of energy.

$$E\ 3-2 \quad \text{Conservation of mass} \rightarrow \nabla \cdot \vec{V} = 0$$

$$E\ 3-3 \quad \text{Conservation of momentum} \rightarrow \rho \frac{D\vec{V}}{Dt} = -\nabla p + \mu \nabla^2 \vec{V} + \rho \cdot \vec{g}$$

$$E\ 3-4 \quad \text{Conservation of energy} \rightarrow \rho \left(\frac{\partial \varepsilon}{\partial t} + v \cdot \nabla \varepsilon \right) + p \nabla \cdot u = \nabla \cdot (K_H \cdot \nabla T)$$

3.2.1 BERNOULLI EQUATION

Bernoulli's equation describes the energy of fluid through its pressure, its height or elevation, and the speed at which it travels. The pressure form of the Bernoulli equation is shown below:

$$E\ 3-5 \quad P + \frac{\rho}{2}V^2 + \rho gh = \text{constant}$$

The equation states that the sum of the pressures or energies of a fluid due to the pressure of the fluid or static pressure, to the dynamic pressure due to the velocity of the fluid, known as kinetic energy per unit volume, and the hydrostatic pressure due to gravity and elevation above a reference level, known as potential energy per unit volume, remains constant along a streamline. That is, the energy of a fluid is conserved along a streamline.

The streamline of a particle can be defined as a curve that is tangent to the velocity vector followed by the particle.

Considering a flow going through a pipe in which cross-area decreases and considering point 1 before the decrease and point 2 after the decrease, shown in Figure 33.

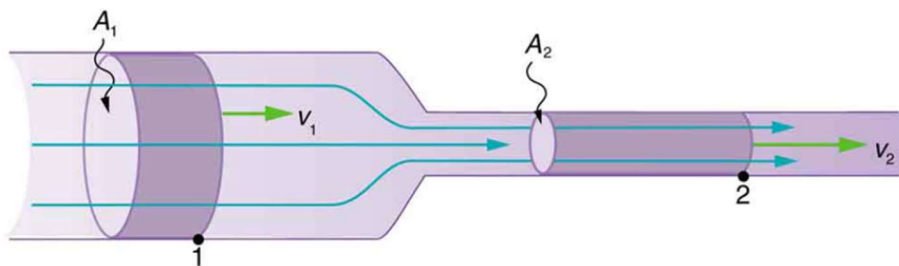


Figure 33: Pipe with decreasing Area

From the conservation of mass, we get what is called the continuity equation, also it will be considered that the fluid is incompressible, an assumption that can be made for a Mach, the relation between the speed of an object and the sound speed in that environment, less than 0.3.

$$E\ 3-6 \quad \dot{m}_1 = \dot{m}_2 \rightarrow \text{Incompressible } (\rho \text{ is constant}) \rightarrow V_1 = \frac{A_2}{A_1} * V_2$$

From Bernoulli's equation we get the next result, considering the same elevation for both points of the study:

$$E\ 3-7 \quad P_1 + \frac{\rho}{2} V_1^2 + \rho gh = P_2 + \frac{\rho}{2} V_2^2 + \rho gh \rightarrow P_1 - P_2 = \frac{\rho}{2} * (V_1^2 - V_2^2)$$

Inserting *E 3-6* into *E 3-7*, we get:

$$E\ 3-8 \quad P_1 - P_2 = \frac{\rho}{2} V_1^2 * \left(\frac{A_1^2}{A_2^2} - 1 \right)$$

Therefore, the so-called Bernoulli principle has just been demonstrated, for a horizontal flow, an increase in the speed of the fluid is accompanied by a decrease in its static pressure. The energy needed to accelerate comes from a decrease in pressure.

However, this equation has certain limitations which must be considered to know if the equation can be used or if we should use the Navier-Stokes equations: it is only valid for a laminar and steady flow, that is, there are no variations in time; losses due to viscous forces are negligible and the fluid is incompressible.

3.3 DRAG AND LIFT

When an object moves through a fluid or vice versa, the fluid exerts a force on the object. This force can be divided into two components: one that acts in the same direction of flow called the drag force, and another that acts in the perpendicular direction of the flow called the lift force. As the fluid that we will treat is air, these forces are called aerodynamic forces.

Aerodynamic forces are due to two types of stresses that act on the surface of an object: first, tangential stresses act as a result of friction between the fluid and the body and are due to the viscosity of the fluid; second, pressure stresses act perpendicular to the surface of the

object and are due to the distribution of pressures around the object. Both stresses can be seen in Figure 34.



Figure 34: Shear and Pressure stresses

3.3.1 DRAG

The drag force, in the case of F1 cars, is an unwanted force. This has a great effect on fuel consumption, which leads to a heavier car as it needs more gasoline, and therefore slower, and in the aerodynamic performance of the car. This is why engineers try to minimize this force.

The drag force is the horizontal component of the aerodynamic forces that the object undergoes. It has two components: pressure drag, due to pressure stresses, and friction drag, due to shear stresses. Its equation is shown below:

$$E\ 3-9 \quad F_D = \int_A (-P \cos\theta - \tau_w \sin\theta) dA$$

Bearing in mind that obtaining the pressure distribution P and the stress distribution X are practically impossible to obtain, the drag equation used is the following:

$$E\ 3-10 \quad F_D = \frac{1}{2} c_D * \rho * v^2 * A$$

Where c_D is the drag coefficient, which represents the effect of the fluid regime as well as the part geometry when generating drag; ρ is the density of the fluid; v is the relative velocity between the fluid and the object, which is assumed to be constant and uniform, and A , a reference area that depends on how the drag coefficient is obtained.

In the case of the front wing, it is about minimizing c_d as much as possible to create a lower drag force. In addition, the reference area used in this case is the front area of the same.

Pressure drag, the first component of the equation, is more significant on blunt bodies. In these the pressure difference between the front, the high-pressure area; and the rear, the low-pressure area, is significant. In addition, this increases significantly if flow separation occurs, at which point the boundary layer of the fluid detaches from the body, creating a trail of recirculating flow in the area called the separation region. Also, in this region, a vortex can appear, creating instability. It is in this area where the turbulent flow decreases the pressure, increasing the pressure difference and therefore the drag force experienced by the object.

As the fluid comes into contact with the object, it accelerates, and therefore, the pressure of the flow decreases. This is a favorable pressure gradient. From a certain point, the flow begins to decelerate, and therefore the pressure increases, appearing as an adverse pressure gradient. This change in the pressure gradient causes the fluid to try to travel in the opposite direction to the flow, and since it cannot be due to the oncoming flow, it detaches from the surface of the object, as shown in Figure 35. If the flow is laminar, it creates more resistance since the separation of the boundary layer appears earlier than in turbulent flow since turbulence carries with it a greater momentum transfer in the fluid, which translates into an increase in the ability to withstand a greater change in the pressure gradient. This is the reason why the aerodynamic shape that generates the least pressure drag is a drop since there is no separation of the boundary layer.



Figure 35: Flow separation

It is precisely in these types of bodies, those with a large surface aligned with the direction of flow, where shear drag, the second component of the equation, is most significant. The

friction drag is proportional to the viscosity of the fluid. Because turbulent flow presents a more drastic change in fluid velocity closer to the object, shear stresses are higher than for laminar flow.

Therefore, by stretching a part in the direction of the fluid, the friction drag increases and the pressure drag decreases, which is why there must be a balance between the two. This explains why the most streamlined body is not the one that produces the least amount of drag. This can be seen in the graph in Figure 36.

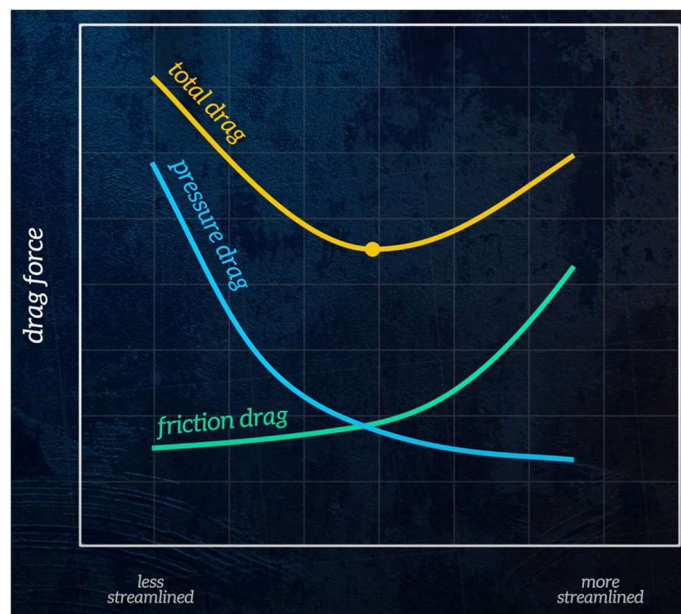


Figure 36: Drag Force vs Streamlining of the Body

3.3.2 LIFT

In the case of F1 cars, the force that is wanted is the opposite of lift, downforce, this increases the grip of the car making it easier to drive and allowing you to corner faster. That is why Formula One engineers try to minimize drag forces while maximizing the downforce created by the car.

The surfaces responsible for generating lift are called airfoils, and these are based on generating a pressure difference between the surfaces perpendicular to the fluid.

To define an airfoil, first of all, you have to describe its leading edge, the edge that is at the beginning; and the trailing edge, the one at the end. The line joining these two edges is called the chord line, and the angle between this line and the direction of airflow is called the angle of attack. Depending on this angle, if it is positive concerning the horizontal in a clockwise direction, the body will generate lift force and if it is negative, it will generate downforce. If the angle of attack is increased, the lift generated is increased. On the other hand, this increase occurs up to an angle of about 60° , after which there is the separation of the boundary layer and, consequently, a drastic reduction in lift and an increase in drag.

The line that passes through the middle of the gap between the upper and lower surfaces and joins the trailing and the leading edge is called the camber line, and it describes the curvature of the airfoil. Both the camber and the angle of attack are parameters that drastically influence the amount of lift that a piece is capable of generating. If we increase the camber of an airfoil, the lift force will increase since more air will be displaced in the vertical direction. However, the drag force will also increase as the frontal area of the part increases. The terminology described above is shown in Figure 37.

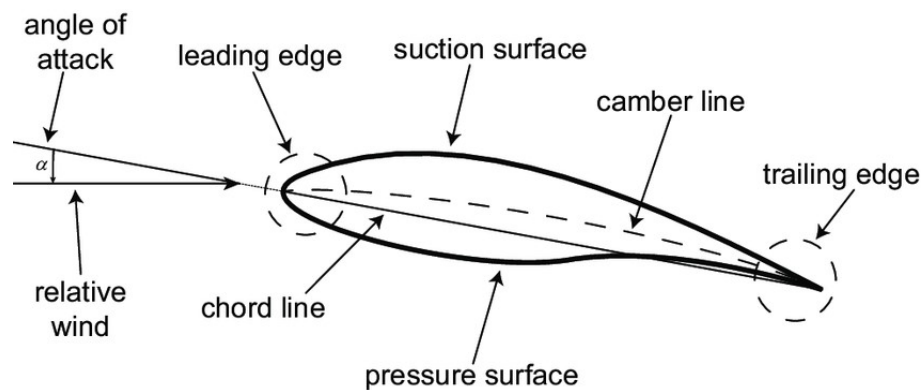


Figure 37: Airfoil Terminology

The lift is the resultant perpendicular to the flow of pressure stresses and friction stresses, which have been explained previously. Its equation is shown below:

$$E\ 3-11 \quad F_L = \int_A (-P \sin\theta - \tau_w \cos\theta) dA$$

As for drag, since the pressure field is impossible to obtain, the following formula is used:

$$E\ 3-12 \quad F_L = \frac{1}{2} c_L * \rho * v^2 * A$$

In this case, c_L is the lift coefficient and deals with the behavior of the fluid as well as the geometry of the part when generating lift, and A is the wing area, in the case of the ailerons, it is calculated by multiplying the wingspan by rope.

In airfoils, the vast majority of lift is due to the pressure field and not to friction, which mostly affects the drag force. This is why symmetrical ailerons with zero angle of attack do not generate lift. Furthermore, most of the force is produced in the zone of negative pressure or subtraction. In turn, the area with the greatest pressure difference, and therefore the greatest force, is in the area where the piece comes into contact with the fluid.

To try to explain the reasons why the lift is generated, there are two approaches: Bernoulli's and Newton's third equation.

Bernoulli's approximation explains that, when the fluid comes into contact with the object at the leading edge, it has zero relative speed, this is the so-called stagnation point. Considering that the fluid that passes through the upper surface (positive angle of attack) accelerates, and since its energy remains constant, ignoring friction, its pressure decreases creating a low-pressure area and, on the other side, the speed decreases creating a high-pressure zone. It is this pressure difference that creates the lift force.

Since the air flows that divide when passing through the object must become parallel, this is the so-called Kutta condition, there must be a circulation around it that accelerates the flow through the upper surface, the zone of greater area, and that decreases its speed in the lower zone.

Newton's approximation is based on the fact that every force has a reaction in the same direction but the opposite direction. Since, in the global computation, an airfoil throws a downward flow of air, the air generates a reaction that drives the airfoil in the opposite direction.

One of the most important aerodynamic coefficients and the one that will be studied in subsequent simulations will be the ratio between the lift coefficient and the drag coefficient as a measure of the aerodynamic efficiency of the wing.

$$E\ 3-13 \quad \text{Aerodynamic efficiency} = \frac{c_L}{c_D}$$

3.4 CFD OPERATION

Fluid modeling through software has become much more powerful in recent years. To the point that the different teams mainly base their studies on Computational Fluid Dynamics, CFD, given the time and capital savings compared to the wind tunnel, where they finally end up verifying that the models obtained in the simulations are correct.

The steps that this software follows are the next: first, it models the fluid around the piece as a mesh of discrete elements; then, boundary conditions and fluid properties need to be described, and after all this process, the Navier-Stokes equations are solved for each element.

The program solves the equations by iteration until a point of convergence has been reached from which the process can be considered finished.

The advantage of CFD over continuous fluid analysis is that thanks to the discretization of the control volume, the equilibrium conditions must only be fulfilled in a discrete number of finite elements, which are interrelated with each other through the nodes that unite them

In addition, depending on the levels of precision needed to solve the problem, we can create a mesh that is more or less refined, considering that the greater the discretization, the greater

the computational power will be required. To look at the levels of precision obtained, we must focus on the residuals of the study.

One of the main problems of the CFD study against the wind tunnel is the absence of movement of the wheels, which means that the flow represented is not exactly the one observed in the wind tunnel due to the absence of the wheel wake.

3.5 WIND TUNNEL OPERATION

As for the wind tunnels, these are an extremely expensive and very important element in the development of the car's aerodynamics. Once the geometries have been tested using CFD and have been found to be satisfactory, they are taken to the wind tunnel for subsequent verification. The number of simulations a team can run is inversely proportional to their position in the constructors' championship from the previous season.

It is logical that the models tested in the wind tunnel are scale models of the original, which is usually 40% or 50%, in order to save capital and time, being 60% the maximum allowed by the FIA. However, there are differences between the effects of the boundary layer between the real model and the scale model. This can be solved by increasing the velocity of the fluid, increasing the Reynolds number and reducing the size of the boundary layer, however today, most installations have a maximum speed of approximately 225 km/h, and it is limited by the FIA to 180 km/h.

It is important to highlight the importance of the mobile floor in the operation of the tunnel, since in this way the reliability of the results obtained will be greater. The basic functions of wind tunnels are: the absorption of air through an opening that contracts and accelerates the speed of the flow and passes through the model, which is supported by a vertical arm. In addition, as is logical, the tape must move at the same speed as the wind to simulate the movement of the vehicle in the closest way to reality.

To prevent the boundary layer from reaching the moving belt, suction is applied through the ground, ahead of the moving belt. The high cost of this system is due to various factors: a

sophisticated belt cooling system that prevents it from heating due to friction and the consequent heating of the air, which would nullify the reliability of the results; the system for raising both the tape, so that it is perfectly attached to the lower area of the car and does not detach due to negative pressure, and the air, so that the flow is ordered; the use of strain gauges attached to the vertical arm that supports the model, as an object for measuring aerodynamic load and drag. In addition, many more gauges are glued to the model to calculate the pressure of these zones. It is for all this that it is estimated that the daily cost of a wind tunnel is around \$14,000. Shown in Figure 38 is the Mercedes team wind tunnel.



Figure 38: Mercedes Wind Tunnel

All this means that the quality of the measurements must be extremely high, especially, when we talk about a sport, in which the time difference between the cars is reduced to thousandths of a second.

On the other hand, the results obtained in the wind tunnel are not always completely reliable, because sometimes the correlation between what is obtained in the wind tunnel and what is seen on the track is not as expected. Another problem of the 2022 season, porpoising, cannot be solved in the wind tunnel because studies with sudden dynamic changes in the height of the cars cannot be carried out.

Chapter 4. CFD SETUP

The objective of the study is to carry out an aerodynamic comparison between the front wings of the Formula 1 cars of the years 2016 and 2022. The study will be carried out through CFD, especially the Fluent module of the ANSYS simulation program. Next, an explanation of the procedures and the setup that has been used for the analysis will be carried out.

4.1 MODEL SELECTION

The models of the wings that are the object of study are not exactly the same as those used by the teams. This is because each of the teams logically goes for a front wing with a slightly different shape to achieve an aerodynamic advantage, and therefore these models are confidential. Finally, the models that will be used for the aerodynamic study are the front wing of the Mercedes W07, the car driven by Lewis Hamilton and Nico Rosberg with which the team won the constructors' and pilots' world championships in 2016; and the front wing of the AMR22 shown in, a single-seater for the Aston Martin team during the 2022 season, driven by Lance Stroll and Sebastian Vettel. Shown below are the cars' CAD next to the real wings in Figure 39 and Figure 40:

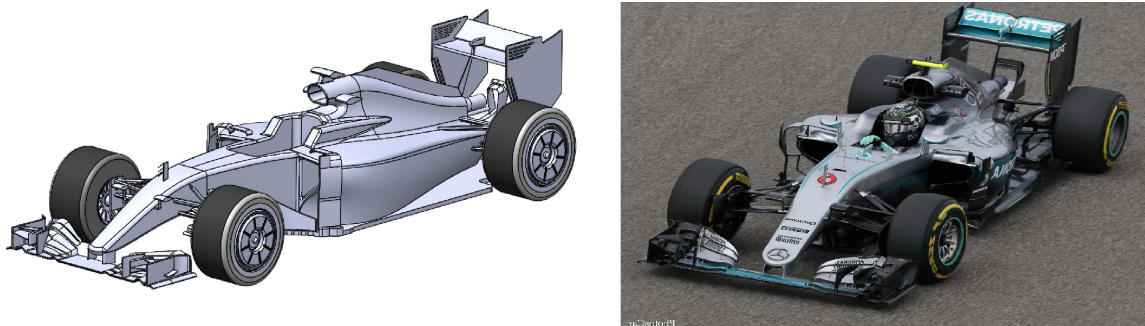


Figure 39: W07 CAD vs Real

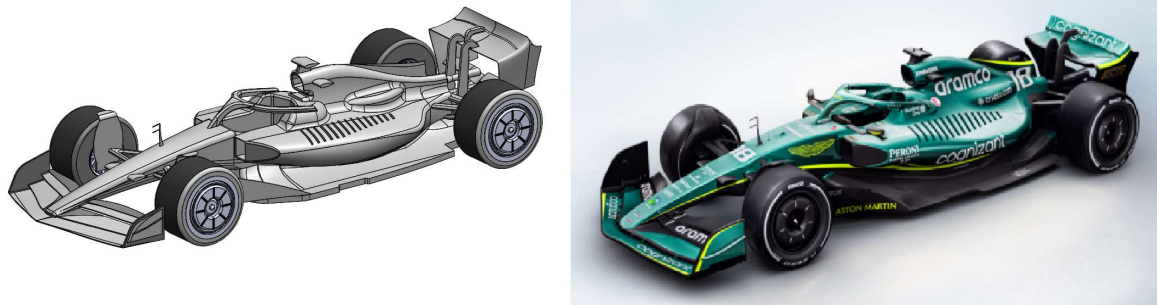


Figure 40: AMR22 CAD vs Real

It should be noted that in this study, the nose of the wing has been included as part of the study since when the front wing is changed in the event of an accident during a race, both the front wing and the nose are changed as a single piece. Shown below are the models of the front wings, extracted from the cars' CAD, next to the real wings in Figure 41 and Figure 42:



Figure 41: W07 Frontwing CAD vs Real



Figure 42: AMR22 Frontwing CAD vs Real

4.1.1 DIFFERENCES BETWEEN CADS AND REAL

As far as the front wing of the W07 is concerned, the main differences are: a smaller curvature in the model in the area outside the vertical flaps; the absence of existing joints

between the flaps, which in turn show their usefulness as secondary vortex generators; lack of curvature in the final tip of the upper flaps, in the area where it joins the main plane; no strakes at the bottom of the wing; and the absence of an ovoid, whose function is the measurement of tire temperature, at the junction with the endplate.

As far as the AMR22's front wing is concerned, the main differences are: the absence of a cavity at the tip of the nose, the function of which is explained in 5.2; a lower curvature of the flaps than usual, this depends on whether the circuit requires a higher top speed, as would be the Monza circuit, and therefore the front section of the wing is reduced, or if it requires more downforce, as would be the Monaco circuit; and the absence of temperature measurer ovoids at the junction with the endplate.

4.2 CONTROL VOLUME AND MESH

To carry out the aerodynamic study, it was necessary, once the geometry of the wing had been obtained, to establish a control volume or flow domain in which the analysis would be carried out. In addition, thanks to the symmetry presented by the pieces, the analysis was carried out with half of the wing and then extended to the other half to save computational power and time.

Thanks to the fact that the dimensions of both ailerons remain similar with a width of 1.8 m and a length of about 0.9 m the control volume used for both ailerons is the same, although the frontal area of the W07 aileron presents a greater frontal area for so you can more easily redirect the airflow. The detailed measurements of the front wing established by the FIA are attached to the drawings in Annex II. It is important to note that the distance that has been established between the lower surface of the front wing itself and the ground has been 275 mm.

It should be noted that for greater accuracy in the results, two control volumes have been created, between which the size of the mesh is differentiated, which decreases as it

approaches the aileron. Shown in Figure 43 are the control volumes that have been applied to both ailerons.

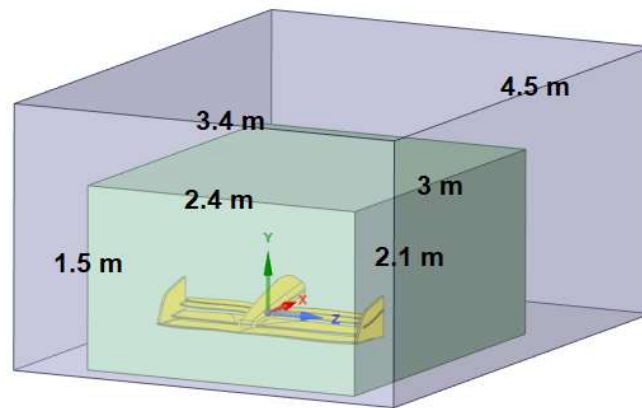


Figure 43: Control Volumes

The flow used for the analysis is an incompressible flow of air in a steady-state, that is, whose speed does not change with time. The incompressibility of it applies since minute variations in air density can be neglected without the results being significantly affected.

As far as meshing is concerned, a volumetric polyhedral mesh has been used. In the largest control volume, the size of the cells has been 500 mm, while in the smallest, a cell size of 150 mm has been established. The object of study, the spoiler has a mesh of 75 mm. Regarding prism layer settings, the smoothing method has been used as a way of meshing variation between the different control volumes and between the control volume and the aileron. Images of the mesh on both wings are shown in Figure 44 and Figure 45.

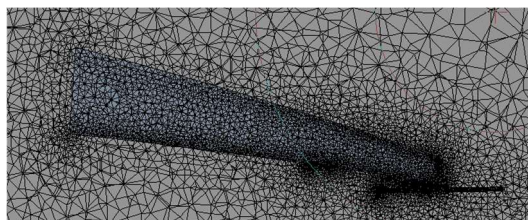


Figure 44: AMR22 Frontwing Mesh

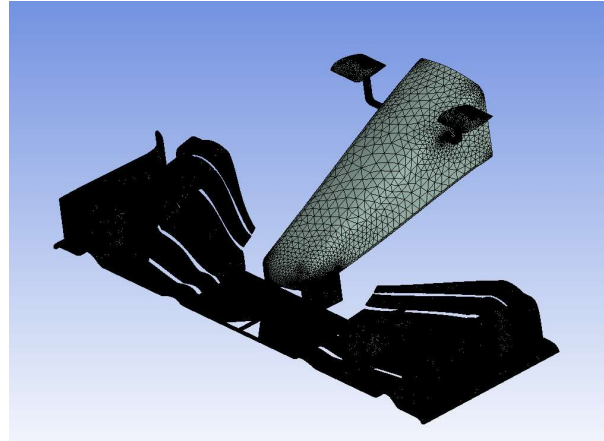


Figure 45: W07 Frontwing Mesh

4.3 CONVERGENCY AND RESIDUALS

The simulations for each of the speeds of both ailerons have been carried out until reaching convergence in the continuity law, which had been established for a value less than $10E-3$. This resulted in 285, shown in Figure 46, iterations for each of the speeds of the AMR22 and 316 for the W07, this higher number of iterations is due to the greater number of cells around the wing resulting from a larger area of this wing.

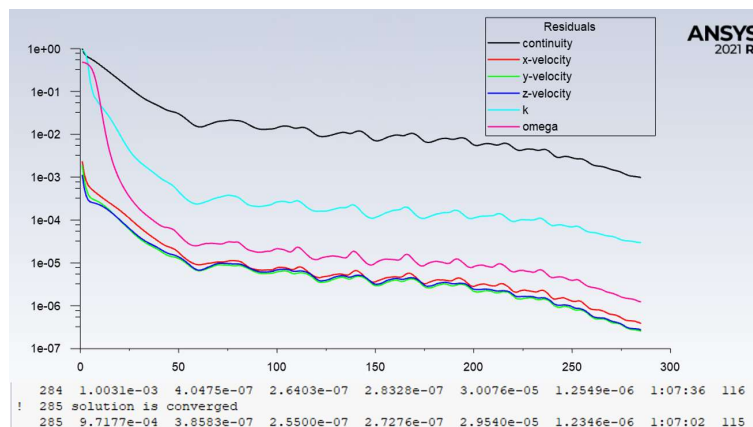


Figure 46: Residuals and Convergency of the Simulations

Chapter 5. ANALYSIS OF THE RESULTS

Once it has been explained how the study has been carried out, we proceed to the analysis of the results obtained once the simulations have been carried out.

This will be carried out at four different speeds: 25, 50, 75, and 100 meters per second. In this way, the efficiency of the ailerons will be studied at each of these speeds, and the speed at which they work optimally. We will especially focus on the analysis for 75 meters per second or 270 kilometers per hour.

5.1 AERODYNAMIC FORCES

It is important to note that in this study the ailerons did not deform as the airflow speed increased, which is beneficial for the aerodynamic efficiency of the study since the compression of the aileron at high speeds decreases the angle of attack. This decrease brings with it a reduction in drag, but not in downforce, since at high speeds there is no detachment of the boundary layer in the lower part of the aileron and therefore it acts as if it had a single flap; considerably increasing the aerodynamic efficiency of the spoiler.

In addition, it was also not possible to simulate the change in height suffered by the wings due to the deformation suffered by the tires as speed increases. This deformation in the tires is because as the speed increases, the downforce increases, and therefore the tires are squeezed against the asphalt, varying the height of the front wing concerning the ground.

It should also be taken into account that due to the ground effect used by the AMR22 single-seater, its efficiency would increase by reducing the distance between it and the asphalt by increasing the pressure difference of what it would do under the spoiler with the air passing freely.

As explained in 2.4, the main function of the front wing is to maximize downforce while trying to decrease drag. This is why it is important to observe how much downforce and drag

both ailerons are capable of generating at each of these speeds, as well as the divergence between them. The values obtained for both simulated ailerons at the four speeds mentioned above are presented in Table 2 and Table 3.

	25 m/s			50 m/s		
	W07	AMR22	Difference	W07	AMR22	Difference
Downforce [N]	237,721	228,510	3,875%	952,256	928,242	2,522%
Drag Force [N]	84,550	42,056	50,259%	338,582	162,323	52,058%

Table 2: Drag and Downforce for 25 and 50 m/s airflow

	75 m/s			100 m/s		
	W07	AMR22	Difference	W07	AMR22	Difference
Downforce [N]	2134,125	2083,390	2,377%	3812,460	3685,420	3,332%
Drag Force [N]	762,507	365,874	52,017%	1355,320	650,377	52,013%

Table 3: Drag and Downforce for 75 and 100 m/s airflow

The differences in terms of lift for each of the speeds are not considerable, with an average difference of 3.026%. Where the differences are considerable are in the drag generated by both wings, which is reduced by an average of 51.586%. This change is due to the differences in the functionalities of both wings. While the old wing, that of the W07, tries to maximize the downforce generated and reduce drag and also seeks a much more complex airflow modification than that of the AMR22.

This airflow modification has two main goals. First of all, avoiding the tires, which is less of a task for the AMR22 wing due to the addition of the over-wheel winglets. Second, the generation of vortices was one of the main causes of the complexity of the ailerons before the change in regulations. These vortices are also responsible for a clear increase in the downforce of the rest of the car, since this front spoiler makes the airflow present in an optimal regime for the rest of the vehicle parts, maximizing its efficiency and sealing the ground.

That is to say, the difference in the drag of the W07 concerning the spoiler of the AMR22 is compensated by an increase in the downforce offered by the other parts of the vehicle thanks to the modification of the airflow through the generation of vortices. In turn, the AMR22 does not need such a complex redirection of the flat bottom due to the return of the flat bottom, which will be responsible for generating most of the downforce of the car.

Once the aerodynamic forces generated by both ailerons have been analyzed, the aerodynamic efficiency generated by each of the ailerons can be studied (view Table 4).

	<i>W07</i>				<i>AMR22</i>			
	25 m/s	50 m/s	75 m/s	100 m/s	25 m/s	50 m/s	75 m/s	100 m/s
CL	2,503	2,507	2,497	2,509	3,912	3,973	3,963	3,943
CD	0,890	0,891	0,892	0,892	0,720	0,695	0,696	0,696
Frontal area (mm2)	303920				186924			
Aerodynamic Efficiency	2,812	2,812	2,799	2,813	5,433	5,718	5,694	5,667

Table 4: Aerodynamic Efficiencies Comparison

As can be seen, the AMR22 has an average aerodynamic efficiency 2 times greater than that of the W07, this is due to the different functionalities between both wings that have been explained previously. In addition, the higher angle of attack required to perform these functionalities makes the W07's frontal wing area 1,626 times larger. Also, it should be noted how aerodynamic efficiency, unlike what happens in reality, does not increase as speed increases, at least considerably. This is because in the study the angle of attack was not varied as we increased the speed of the airflow. This concept is called flexi-wing. The amount of

deformation allowed in both the front wing and the rear wing is regulated by the FIA; thus limiting the advantage that teams can gain from this event. This is shown in Figure 47.

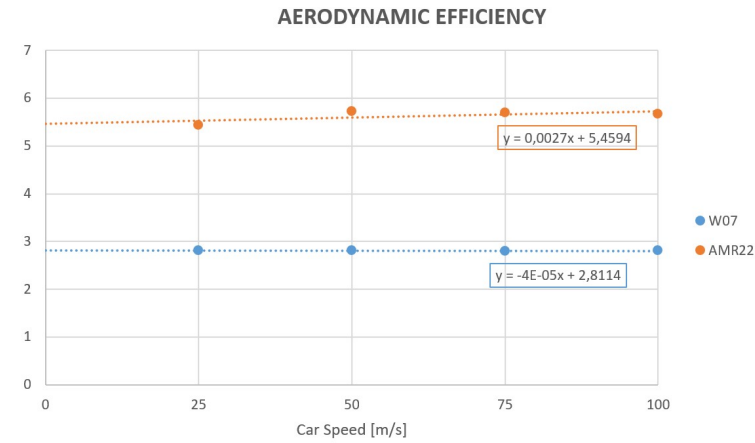


Figure 47: Aerodynamic Efficiency vs Car Speed

5.2 VELOCITY AND PRESSURE DISTRIBUTIONS

To carry out the study of the speeds of the airflow through the fins, it has been decided to cut each fin at 0.7 meters from its axis of symmetry. Once the cuts have been obtained with the plane, the airfoils of both ailerons have been obtained and the variation suffered by airflow at 75 meters per second when in contact with the ailerons has been studied.

As can be seen in the following images, the fluid has been accelerated in the low-pressure area, that is, on the lower surface of the spoiler, and it has been slightly decreased on the upper surface of the spoiler. This agrees with what was explained in 3.2.1 because the pressure decreases on the lower surface of the airfoil and increases on the upper one, the fluid accelerates in the lower area and decelerates in the upper face, remaining constant. the energy of the fluid and generating a downforce that pushes the rest of the car with the ground. The images of the velocity distributions through the ailerons are presented in Figure 48 and Figure 49.

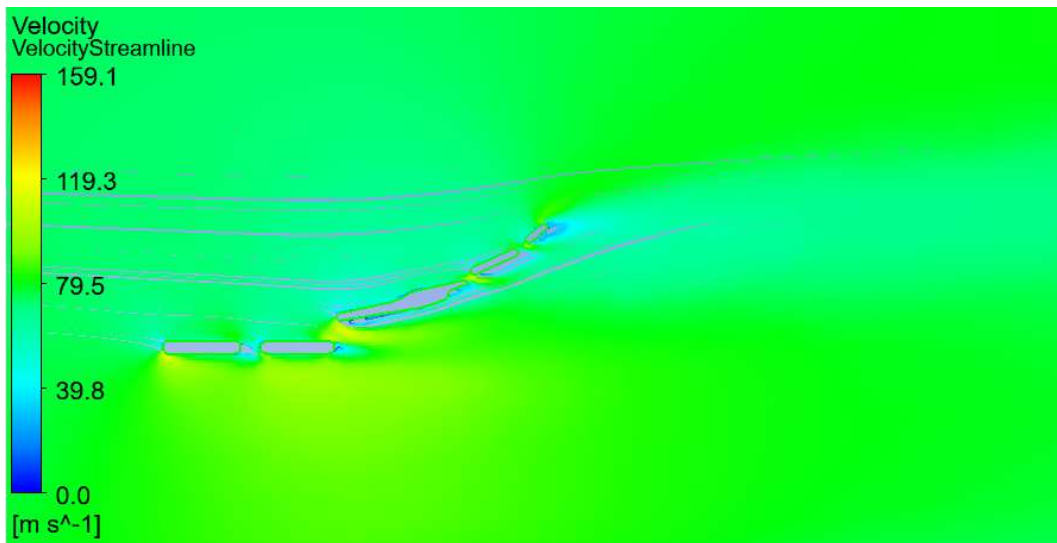


Figure 48: W07 Frontwing Velocity Streamline

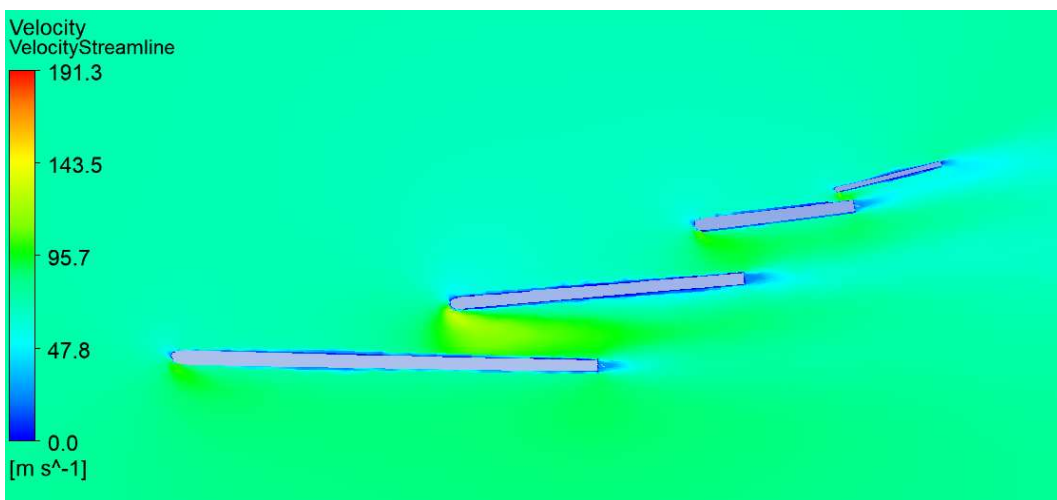


Figure 49: AMR22 Frontwing Velocity Streamline

In addition, the fluid is strongly decelerated once it finishes running through the flap. This deceleration can end up resulting in the separation of the boundary layer, as is the case of the two upper flaps of the W07, an area in which the drag increases considerably due to the increase in turbulence on the rear face of the aileron.

You can also see how the no-slip condition has been added to both wings, being especially visible on the front wing of the AMR22. In this, a sheet of air with zero speed is presented through each flap.

This is ratified once we observe the pressure distributions in both ailerons, in which we can observe a zone of higher pressures on the upper face and lower pressures on the lower face. In turn, it should be noted that the pressure distribution in the front wing of the W07 is much more complex than that of the AMR22 due to the greater complexity of its geometry.

In addition, it can be seen in Figure 50 and in Figure 51 which are the areas of the spoiler that suffer a greater pressure difference and, therefore, a greater deformation. For example, the largest flap of the W07, the third starting from the lower aileron, is the one with the greatest pressure difference. In turn, this pressure difference is visible at the end of the W07 endplate, an area in which the fluid is spat out of the car.

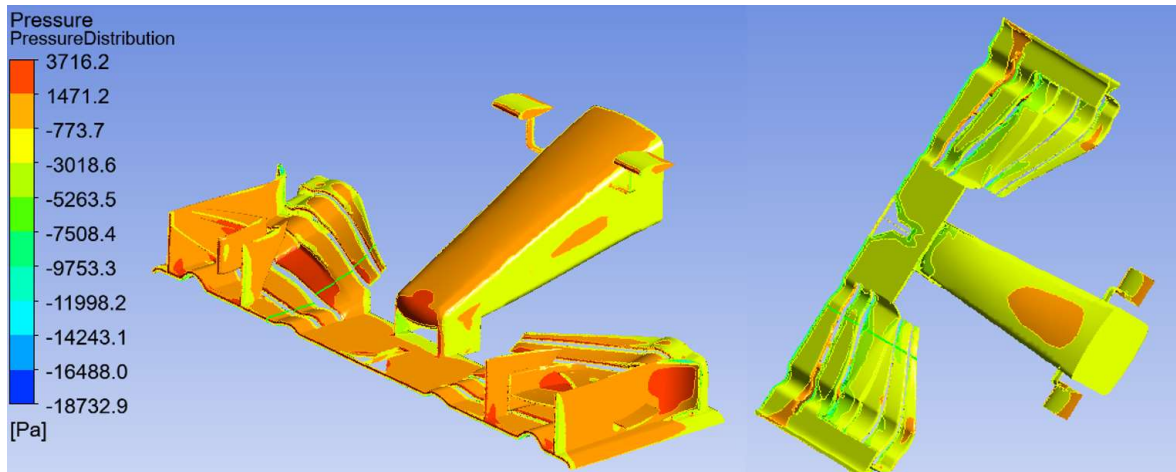


Figure 50: W07 Frontwing Pressure Distribution

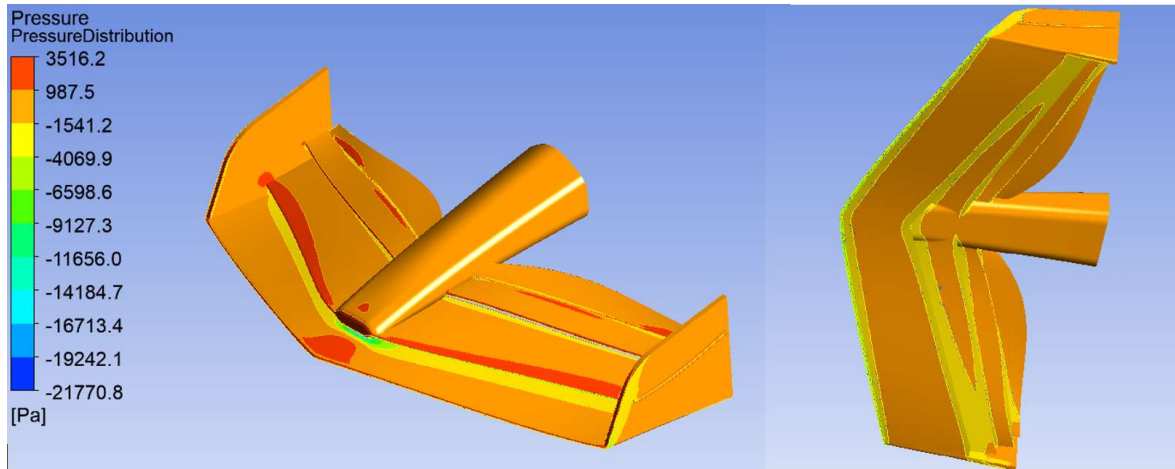


Figure 51: AMR22 Frontwing Pressure Distribution

It is worth noting the high pressures that appear at the tips of the noses of both wings, an area in which a stagnation point is created, this problem has been shown with a common solution among the teams. The creation of a cavity at the tip of the nose reduces the high pressures suffered by this area. This was included by all the teams after the Ferrari team with its F1-75 showed this solution during the preseason in Barcelona. Therefore, the current AMR22 spoiler has a cavity at its tip, shown in Figure 52 while the model obtained for the analysis was obtained immediately after the presentation of the single-seater, at which time it did not have the cavity. In addition, it is speculated that this cavity could be used as an F-duct, which is about manipulating the flow of air inside the car, expelling it in specific areas for greater aerodynamic efficiency, as well as using it as a system of refrigeration of it.



Figure 52: F1 Front Wings' Cavities

During other years the solutions to this problem have been very varied by the different teams. Figure 53 shows everything from solutions based on increasing the height of the nose concerning the rest of the spoiler, to the creation of hollow tips to reduce the high pressures suffered by this part.



Figure 53: Stagnation Point Solutions in F1

5.3 C_p COEFFICIENT

The pressure coefficient is a non-dimensional number which describes the relative pressure through a flow field in fluid dynamics.

$$E\ 5-1 \quad c_p = \frac{p - p_0}{\frac{1}{2} * \rho * V^2}$$

Where p is the pressure of the surfaces, p_0 is the ambient pressure, ρ is the density of the fluid that runs through the surface, and V is the relative speed between the fluid and the surface.

This coefficient is especially useful since the lift coefficient depends directly on it. Being proportional to the integral of the difference in pressure coefficients between the upper face and the lower face of the airfoil. The existing relationship is presented below:

$$E\ 5-2 \quad C_l = \frac{1}{x_{TE} - x_{LE}} * \int_{x_{LE}}^{x_{TE}} (C_{pl}(x) - C_{pu}(x)) dx$$

The profile of the studied ailerons is the same as that presented in the speed profiles. That is why in Figure 54 5 curves are seen due to the 5 flaps and in Figure 55 4 curves are seen due to the 4 flaps.

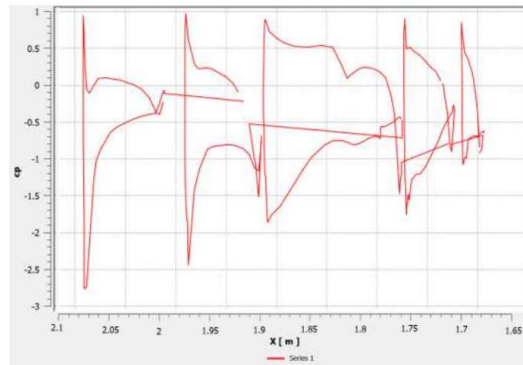


Figure 54: W07 Frontwing c_p coefficient

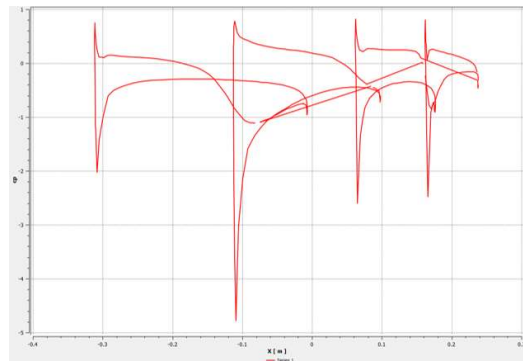


Figure 55: AMR22 Frontwing c_p coefficient

As can be seen in Figure 54, its flaps present the greatest pressure difference at the end of each of them. The flap that generates the most downforce is the third, the one with the largest surface area and with the highest difference in pressures.

On the other hand, the flaps of the AMR22 generate most of the downforce, where the greatest pressure difference occurs, in their initial zone. The flap that generates the most

downforce is the second, which is logical because it is also the one with the largest surface area.

5.4 WAKE STRUCTURE AND VORTICITY

As can be seen in the following images, the airflow created by the front wing of the AMR22 is much more orderly than that of the W07, this is due to the greater simplicity in the geometry of the part. Both generate large vortices in the area where the flaps join the endplate, however, this is much weaker since the vertical flaps try to expel air out of the car, producing a clash between both flows and weakening the vortex. In addition, you can see the formation of the Y-250 vortex in the front wing of the W07, it is located at the junction of the flaps with the main plane, exactly 250 millimeters from the midplane. This was one of the most important vortexes in the aerodynamics of the old cars, but with the change in regulations and the attachment of the flaps directly to the nose of the car, this vortex disappears. The front view of the airflow through both wings is shown in Figure 56 and Figure 57.

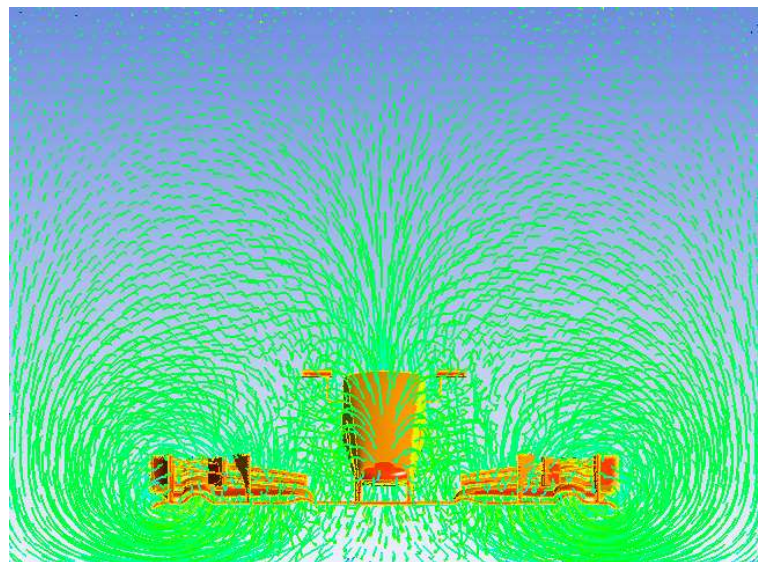


Figure 56: Wake of the Airflow for W07 Frontwing

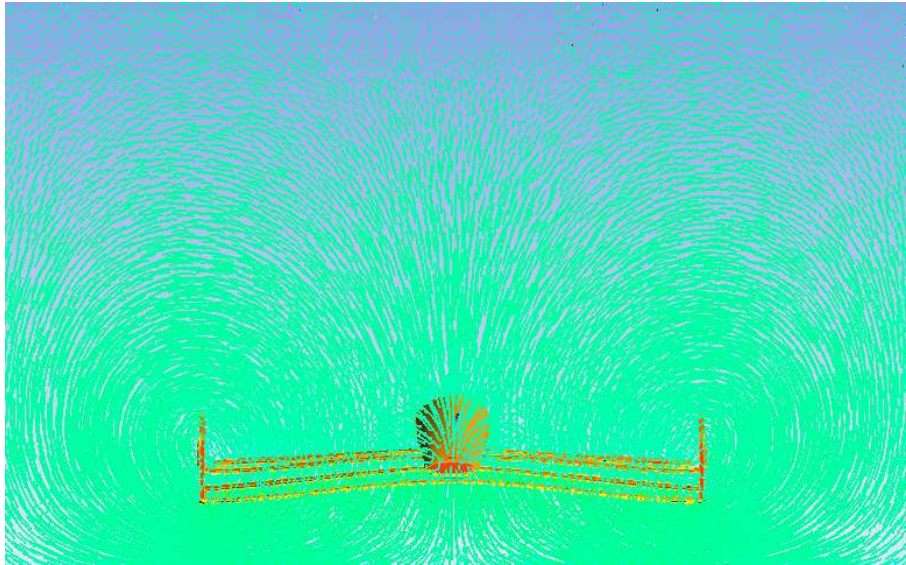


Figure 57: Wake of the Airflow for AMR22 Frontwing

To carry out a study of the vortices that are generated at the rear of both wings, and their comparison, the behavior of the total pressure field has been studied, thus taking into account both the static pressure and the dynamic pressure, and also the speeds of the flow behind the flaps. These can be seen in Figure 58, Figure 59, Figure 60, and Figure 61.

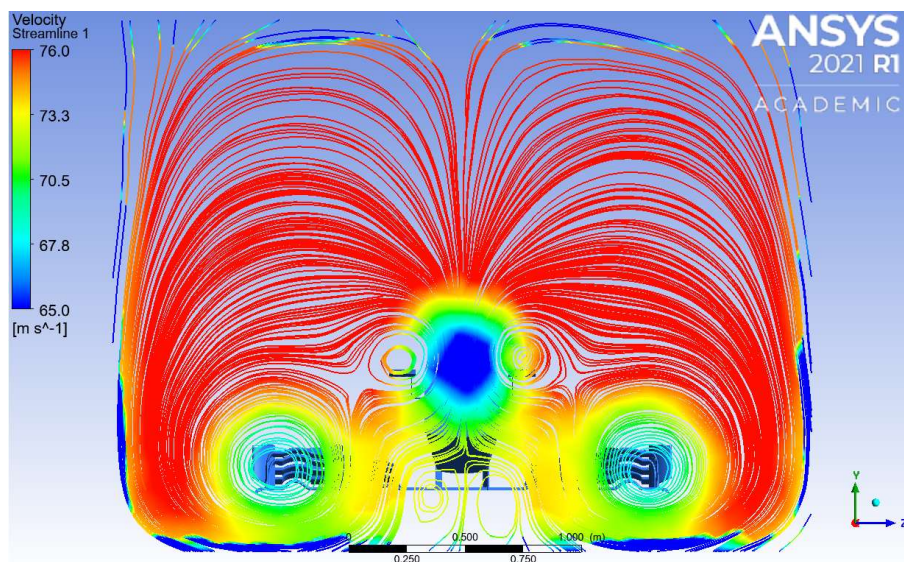


Figure 58: Flow Speed behind W07 Front Wing

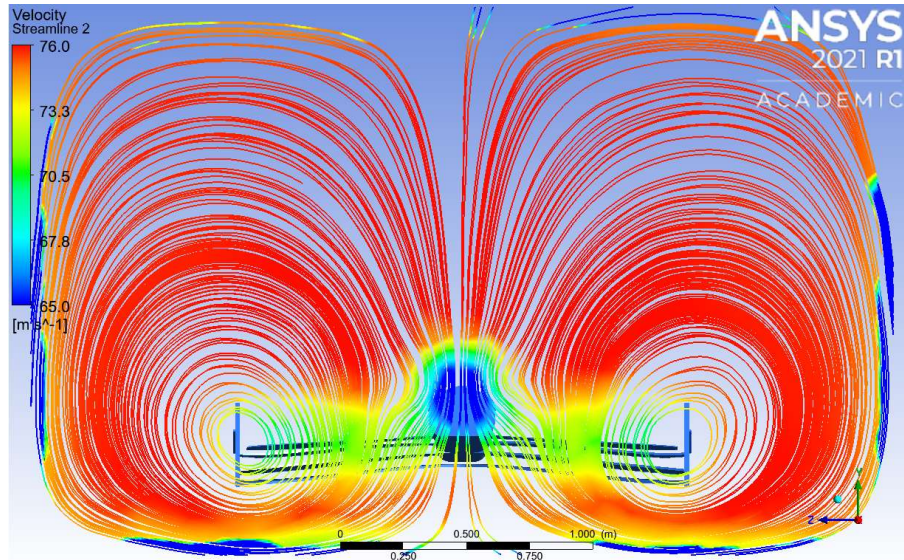


Figure 59: Flow speed behind AMR22 Front Wing

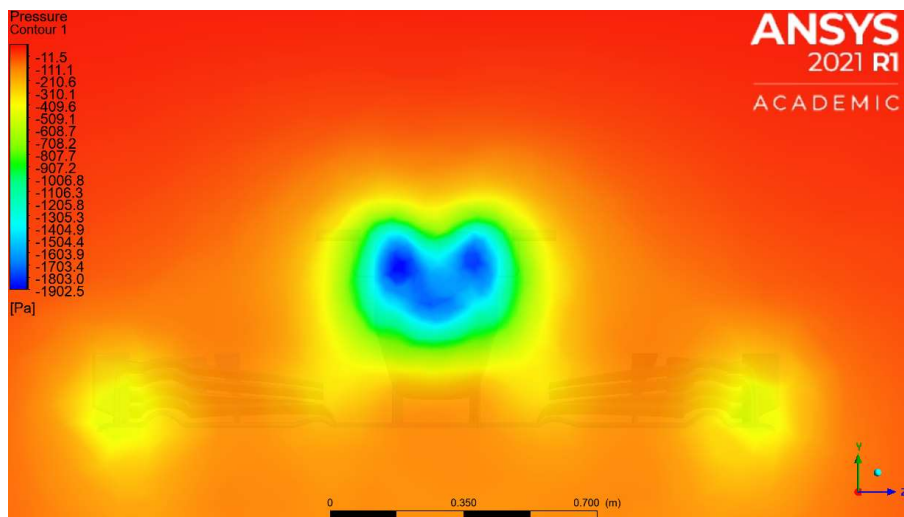


Figure 60: Total Pressure Field behind W07 Front Wing

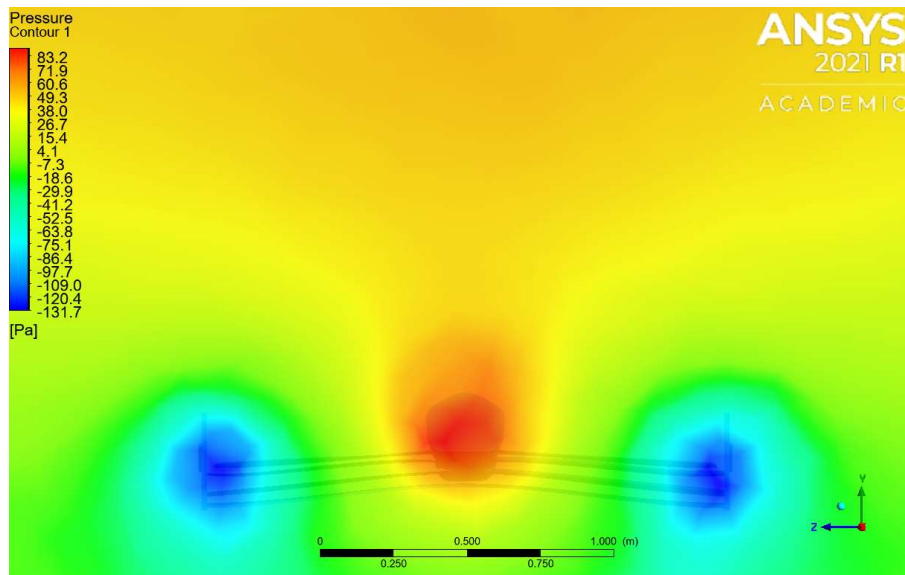


Figure 61: Total Pressure Field behind AMR22 Front Wing

As can be seen in these images, the complexity of the vorticity is very different. Many more vortices can be seen on the wing of the W07, the functions of which are explained below.

In the first place, the vortex that we found between the area where the nose meets the main plane and the area where the flaps meet the main plane is presented. This is called vortex Y-250, and it was the most important vortex until the arrival of the change in regulations. This receives this name since it starts exactly 250 mm from the central plane of the car. The function of this was the expulsion of the wake generated in the middle area of the wheel from its inner face, outwards, so that the rest of the car's aerodynamics work optimally. In turn, this is responsible for sealing the flat bottom. The bargeboards redirect it towards the outer zone of the flat bottom, acting as a barrier and enhancing the ground effect.

The small vortices generated in the upper area of the nose are due to the small fins that are on it. Its function is to try to order as much as possible the turbulent airflow created by the halo and by the pilot's inlet cavity and the pilot's head.

On the other hand, the vortices generated in the endplate, in the case of the W07, are more powerful than in the AMR22 due to the vertical flaps, which have the function of expelling the airflow from the outer area of the wheel.

All these vortices try to minimize the damage of the front wheel wake on the aerodynamics of the rest of the car while maximizing the car's downforce. In the case of the AMR22, the wheel winglets and the new floor of the car come to play an important role, largely replacing the role of the vortices and achieving a more orderly airflow behind the car.

5.5 RELIABILITY OF THE RESULTS

"All models are wrong, but some are useful", one of the most famous aphorisms of the statistician George Box. As far as results are concerned, the results obtained through the CFD will never exactly coincide with those obtained in the wind tunnel, this is due to all the simplifications and assumptions that we carry out before carrying out the analysis. Instead, the important thing is to reduce this margin of error concerning reality as much as possible and, understand the mathematical models extracted from fluid mechanics on which CFD is based, to know when we can trust the results obtained or when we should be more skeptical.

Chapter 6. ENVIRONMENTAL IMPACT

For this section, we will carry out a study of the equivalent of carrying out an aerodynamic study exclusively through CFD technology and instead of having done it through an owned wind tunnel. A study of the reduced carbon footprint in terms of kilograms of CO₂ emitted will be carried out, and the Sustainable Development Goals (SDGs) that have been met will be mentioned and explained.

First of all, we will mention the materials and energy necessary to study the front wing in a wind tunnel: we would need the matrix or chassis and the front wing, both aluminum parts and climbed to 40%, the operation of the wind tunnel for 1 hour, with all that, entails, that is, the operation of the turbine, the belt, the cooling system and the use of, 12 strain gauges, 2 in the vertical arm, another 10 distributed around the rest of the spoiler and finally, subsequent post-processing of the data for 3 hours on a computer. For the calculation of the carbon footprint, the pollution emitted due to the transport, extraction, and machining of the different materials will not be considered; just like the sum of the CO₂/equivalent use will not be considered.

We then proceed to the presentation of the data obtained and even later calculation of the carbon footprint produced by the wind tunnel.

Data:

- Actual chassis weight = 126 kg
- Actual front wing weight = 14.45 kg
- Carbon fiber density = 1750 kg/m³
- Aluminum density = 2700 kg/m³
- kg CO₂ eq/ kg aluminum = 1.5 (in the USA)
- Energy used by the wind tunnel = 4000 kWh
- Energy used by the computer = 0.4 kWh

- kg CO₂ eq/ kWh = 0.433 (in the USA)
- Strain gauge = 1 kg CO₂/ gauge (estimated)

$$E\ 6-1 \quad \text{Chassis } CO_2 = 126 \text{ kg cf} * \frac{2700 \frac{\text{kg al}}{\text{m}^3}}{1750 \frac{\text{kg cf}}{\text{m}^3}} * 0.4 * 1.5 \frac{\text{kg } CO_2}{\text{kg al}} = 116.64 \text{ kg } CO_2$$

$$E\ 6-2 \quad \text{Front wing } CO_2 = 14.45 \text{ kg cf} * \frac{2700 \frac{\text{kg al}}{\text{m}^3}}{1750 \frac{\text{kg cf}}{\text{m}^3}} * 0.4 * 1.5 \frac{\text{kg } CO_2}{\text{kg al}} = 13.37 \text{ kg } CO_2$$

$$E\ 6-3 \quad \text{Energy } CO_2 = \left(4000 \frac{\text{kW}}{\text{hr}} * 1\text{hr} + \frac{0.4\text{kW}}{\text{hr}} * 3\text{hr} \right) * 0.433 \frac{\text{kg } CO_2}{\text{kW}} = 1732.52 \text{ kg } CO_2$$

$$E\ 6-4 \quad \text{Gauges } CO_2 = 1 \frac{\text{kg } CO_2}{\text{gauge}} * 12 \text{ gauges} = 12 \text{ kg } CO_2$$

$$E\ 6-5 \quad \text{Wind tunnel } CO_2 = 1874.53 \text{ kg } CO_2$$

In the case of the CFD study, the only necessary component is a computer, and it will be estimated that the time of calculation, setting, and subsequent post-processing of the data for each of the speeds is 4 hours.

We then proceed to calculate the carbon footprint produced by the CFD study.

$$E\ 6-6 \quad \text{CFD } CO_2 = 0.4 \frac{\text{kW}}{\text{hr}} * 4 \frac{\text{hr}}{\text{velocity}} * 4 \text{ velocities} * 0.433 \frac{\text{kg } CO_2}{\text{kW}} = 2.77 \text{ kg } CO_2$$

Therefore, the savings in CO₂ are 1871.76 kg. As it can be seen the savings, in terms of the equivalent amount of CO₂ are considerable, at 99.84% specifically. In addition, this reduction complies with SDG number 13, which is explained below.

- SDG 13: Immediate urgent action to combat climate change and its effects. By reducing the kg of CO₂ equivalent by 99.85%, it follows that this goal is met

Chapter 7. ECONOMIC ANALYSIS

For this section, we will carry out a study of the equivalent of carrying out an aerodynamic study exclusively through CFD technology instead of having done it through our wind tunnel.

The materials are the same as those mentioned in Chapter 6. considering that, for the wind tunnel you need a wind tunnel engineer and a machinist in charge of designing the models, and that for the study of CFD a CFD engineer is needed. It is worth mentioning that for the economic calculation the cost of transporting the materials or modeling them will be considered.

The data of interest for the economic study of wind tunnel analysis, then the calculation of it, are shown below.

Data:

- Aluminum = 86.67 kg
- Wind tunnel engineer = 40 \$/hr
- Machine operator = 14.5 \$/hr
- Machining hours = 20 hr (estimated)
- \$/ kg aluminum = 3.4 (in the USA)
- Energy used by the wind tunnel = 4000 kWh
- Energy used by the computer = 0.4 kWh
- \$/ kWh = 0.2 (in the USA)
- Strain gauge = 170 \$/ gauge (estimated)

E 7-1

$$\text{Aluminum } \$ = 86.67 \text{ kg al} * 3.4 \frac{\$}{\text{kg al}} = 294.70 \$$$

$$E\ 7-2 \quad \text{Energy } \$ = (4000 \frac{kW}{hr} * 1hr + 0.4 \frac{kW}{hr} * 3hr) * 0.2 \frac{\$}{kW} = 800.24 \$$$

$$E\ 7-3 \quad \text{Staff } \$ = 40 \frac{\$}{hr} * (1hr + 3hr) + 14.5 \frac{\$}{hr} * 20\$ = 450 \$$$

$$E\ 7-4 \quad \text{Strain gauges } \$ = 12 \text{ gauges} * 170 \frac{\$}{\text{gauge}} = 2040 \$$$

$$E\ 7-5 \quad \text{Wind tunnel } \$ = 294.70 \$ + 800.24 \$ + 450 \$ + 2040 \$ = 3584.94 \$$$

Next, we proceed to carry out the economic study of the analysis by CFD, and we will consider that the hourly price of the CFD engineer is 43 \$/ hr.

$$E\ 7-6 \quad \text{Energy } \$ = 0.4 \frac{kW}{hr} * 4 \frac{hr}{\text{velocity}} * 4 \text{ velocities} * 0.2 \frac{\$}{kW} = 1.28 \$$$

$$E\ 7-7 \quad \text{Staff } \$ = 43 \frac{\$}{hr} * 4 \frac{hr}{\text{velocity}} * 4 \text{ velocities} = 688 \$$$

$$E\ 7-8 \quad \text{CFD } \$ = 1.28 \$ + 688 \$ = 689.28 \$$$

As can be seen, capital savings are also considered important, with a reduction of \$2895.66, or 80.77%. That is why capital savings when carrying out studies using CFD technology is considered so important, and also, that is why teams with economic problems throughout history have had to reduce the number of wind tunnel hours used in the design of single-seaters.

Chapter 8. CONCLUSIONS AND FUTURE WORKS

The conclusions obtained once the aerodynamic study of the different ailerons has been carried out are as follows. First off, the front wing on the W07 generates roughly the same amount of downforce on its own as the wing on the AMR22. Instead, it generates a much higher amount of drag, due to its greater complexity. This is not to say that the W07 wing is worse than the AMR22 wing the first wing generates a large amount of downforce on the rest of the car thanks to the vortices it generates due to the difficulty of its geometry that the AMR22 is not capable of generating. This is why the new ground through ground effect plays an important role since it must create the aerodynamic load that was previously created by the vortices of the front wing and which have disappeared. In turn, analyzing the complexity of the airflow at the rear of the spoiler, the change in regulations is shown to be effective. It is this same simplification in geometry that brings about a much neater airflow at the rear of the wing, thereby reducing the amount of dirty air generated and allowing for better racing.

In other words, the functionality of the front wings has changed in these successive regulatory changes. The W07's wing sacrifices some of its aerodynamic efficiency in exchange for producing much more in other parts of the car, generating a dirtier airflow. While that of the AMR22 maximizes energy efficiency since the rest of the aerodynamic load is generated on the floor of the car.

On the other hand, it has been concluded that carrying out the aerodynamic study of a front wing using CFD technology, instead of a wind tunnel, drastically reduces the carbon footprint and the capital used, this being reduction of one, respectively. However, the reliability of the results will never be the same given that the models, as models that they are, do not represent reality in its entirety. Finding important differences such as the absence of the wheel wake in the study using CFD.

Chapter 9. BIBLIOGRAPHY

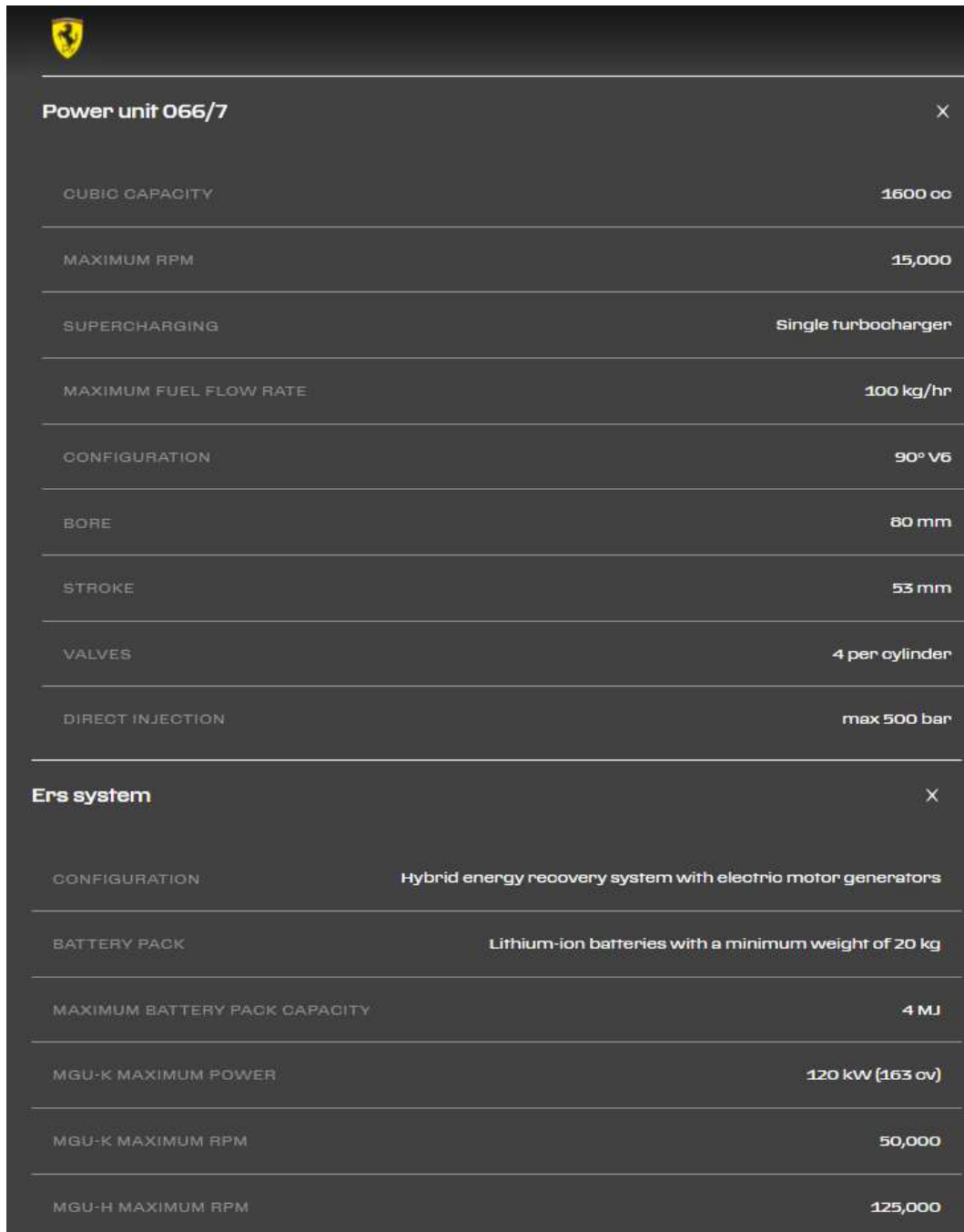
- [1] Adrian Newey, chief technical officer, and aerodynamicist of Red Bull Racing. “How to build a car?”. November, 2017.
- [2] Andrew de Souza. “Race to Perfection”, a docu-series commemorating the 70th anniversary of Formula 1.
- [3] David Penner. “Simulating the William FW43B (AR)”. November, 2021.
<https://www.linkedin.com/pulse/simulating-williams-fw43bar-part-1-all-simulations-wrong-david-penner/?trackingId=Zmvr%2FRzCW3NIBgzC%2FXjBmw%3D%3D>
- [4] Fawaz Bukht Majmader. Front Wing CAD: “Aston Martin AMR22”. February, 2022.
<https://grabcad.com/library/aston-martin-amr22-1>
- [5] Fawaz Bukht Majmader. Front Wing CAD: “Mercedes W07 Hybrid F1 Car”. September, 2021. <https://grabcad.com/library/mercedes-w07-hybrid-f1-car-1>
- [6] FIA Youtube Channel. “FIRST LOOK: Formula 1’s 2021 car in the wind tunnel”. August, 2019. https://www.youtube.com/watch?v=sn2eisHLwwk&ab_channel=FIA
- [7] FIA. “2021 Formula 1 Technical Regulations”. June, 2020.
https://www.fia.com/sites/default/files/2021_formula_1_technical_regulations_-_iss_5_-_2020-06-19_1.pdf
- [8] FIA. “2022 Formula 1 Technical Regulations”. March, 2020.
https://www.fia.com/sites/default/files/2022_formula_1_technical_regulations_-_iss_1_-_2020-03-30.pdf
- [9] F1 webpage. “F1’s revolutionary 2021 rulebook – The thinking behind the changes”. October, 2019. <https://www.formula1.com/en/latest/article.f1s-revolutionary-2021-rulebook-the-thinking-behind-the-changes.7cHf6WKM5FvCIZSPwhwvZ.html>
- [10] F1 webpage. “Analysis - Mercedes’ mystery ‘S-duct’”. November, 2015.
<https://www.formula1.com/en/latest/technical/2015/11/analysis---mercedes-mystery-s-duct.html>
- [11] F1 Youtube Channel. “Everything You Need To Know About The 2022 F1 Car”. July, 2021. https://www.youtube.com/watch?v=hBmWJOy9vT4&ab_channel=FORMULA1

- [12] Greg Stuart. “10 things you need to know about the all-new 2022 F1 car”, F1 webpage. July, 2021. <https://www.formula1.com/en/latest/article.10-things-you-need-to-know-about-the-all-new-2022-f1-car.4OLg8DrXyzHzdoGrbqp6ye.html>
- [13] Greg Stuart. “10 ways the 2021 rules will improve F1”, F1 webpage. October, 2019. <https://www.formula1.com/en/latest/article.10-ways-the-2021-rules-will-improve-f1.1QlkNWf57I3HIAVeVeydyS.html>
- [14] John Anderson, Professor Emeritus in the Department of Aerospace Engineering at the University of Maryland. “Fundamentals of Aerodynamics”. March, 2016.
- [15] Joseph Katz. “Race car Aerodynamics”. January, 1991.
- [16] Lawrence Barretto. “Flexi wings – What are they and why is everyone talking about them?”. May, 2021. <https://www.formula1.com/en/latest/article.flexi-wings-what-are-they-and-why-is-everyone-talking-about-them.3NeugNG480UtFMzy77XKiQ.html>
- [17] Lawrence Barretto. “The 2021 F1 cost cap explained – what has changed, and why?”, F1 webpage. May, 2020. <https://www.formula1.com/en/latest/article.the-2021-f1-cost-cap-explained-what-has-changed-and-why.5OITe8udKLmkUI4PyVZtUJ.html>
- [18] Lluís Llurba. Redbull webpage: “¿Qué impide que un F1 salga volando?”. April, 2017. <https://www.redbull.com/es-es/formula-uno-carga-resistencia-aerodinamica-alerones-historia>
- [19] Marcelo Adotti. AerodinamicaF1 webpage. “Alerón delantero 2020: Análisis aerodinámico”. <https://www.aerodinamicaf1.com/2020/07/aleron-delantero-2020-analisis-aerodinamico/>
- [20] Mario Fernández Osma. AerodinamicaF1 webpage. “El alerón delantero en la F1”. <https://www.aerodinamicaf1.com/aerodinamica-en-la-formula-1/el-aleron-delantero/>
- [21] Mario Fernández Osma. AerodinamicaF1 webpage. “Historia de la aerodinámica en la F1”. September, 2019. <https://www.aerodinamicaf1.com/2019/09/historia-de-la-aerodinamica-en-la-f1/>
- [22] Mario Fernández Osma. AerodinamicaF1 webpage. “Los generadores de vórtices en la Fórmula 1”. October, 2019. <https://www.aerodinamicaf1.com/2019/10/los-generadores-de-vortices-en-la-formula-1/>
- [23] Mario Fernández Osma. AerodinamicaF1 webpage. “Reglamento 2022 – Efecto en la aerodinámica”. November, 2019. <https://www.aerodinamicaf1.com/2019/11/reglamento-2022-efecto-en-la-aerodinamica/>

- [24] Mario Fernández Osma. AerodinamicaF1 webpage. “Teoría”. Abril, 2020.
<https://www.aerodinamicaf1.com/teoria/>
- [25] Matt Somerfield & Giorgi Piola. “Banned: Why McLaren’s F-duct was outlawed”. April, 2020. <https://www.motorsport.com/f1/news/banned-technical-analysis-f-duct/4782715/>
- [26] Matt Somerfield & Giorgi Piola. “Banned: The double diffuser that triggered an F1 development race”. May, 2020. <https://www.autosport.com/f1/news/banned-the-double-diffuser-that-triggered-an-f1-development-race-4982556/4982556/>
- [27] Matt Somerfield & Giorgi Piola. “What’s behind Williams’ unique sidepod hole”. March, 2022. <https://www.motorsport.com/f1/news/whats-behind-williams-unique-f1-sidepod-hole/8599980/>
- [28] Máximo Sant. Garaje Hermético Youtube Channel.
<https://www.youtube.com/c/GarajeHerm%C3%A9tico>
- [29] McLaren webpage. “Dirty Air”. <https://www.mclaren.com/racing/f1-playbook/dirty-air/>
- [30] Racing Atmosphere webpage. “El alerón delantero en la F1”. August, 2018.
<https://www.racingatmosphere.com/aerodinamica/aleron-delantero/>
- [31] Racing Atmosphere webpage. “El efecto suelo en la F1”. August, 2018.
<https://www.racingatmosphere.com/aerodinamica/efecto-suelo/>
- [32] Racing Atmosphere webpage. “¿Qué es un bargeboard en la Fórmula 1?”. August, 2018.
<https://www.racingatmosphere.com/aerodinamica/bergeboard/>
- [33] Rajesh Bhaskaran, Cornell University. “A Hands-on Introduction to Engineering Simulations: Computational Fluid Dynamics”. November, 2021.
https://www.edx.org/es/course/a-hands-on-introduction-to-engineering-simulations?index=spanish_product&queryID=af62475a0c24571a2fe910602aca81df&position=1
- [34] Scott Mansell. Driver 61 Youtube Channel. <https://www.youtube.com/c/Driver61>
- [35] Simon McBeath. “Competition car Aerodynamics”. February, 2013. P73-158.
- [36] The Efficient Engineer Youtube Channel.
<https://www.youtube.com/c/TheEfficientEngineer>
- [37] Thomas Oggioni, Mechanical Design Engineer at Scuderia Ferrari. “Aerodynamics of Formula One Front Wing and its Evolution”. March, 2019.
<https://www.linkedin.com/pulse/aerodynamics-formula-one-front-wing-its-evolution-thomas-oggioni/>

- [38] Wikipedia webpage. “History of Formula 1”. March, 2022.
https://en.wikipedia.org/wiki/History_of_Formula_One

ANNEX I



Power unit 066/7		X
CUBIC CAPACITY		1600 cc
MAXIMUM RPM		15,000
SUPERCHARGING		Single turbocharger
MAXIMUM FUEL FLOW RATE		100 kg/hr
CONFIGURATION		90° V6
BORE		80 mm
STROKE		53 mm
VALVES		4 per cylinder
DIRECT INJECTION		max 500 bar
Ers system		X
CONFIGURATION	Hybrid energy recovery system with electric motor generators	
BATTERY PACK	Lithium-ion batteries with a minimum weight of 20 kg	
MAXIMUM BATTERY PACK CAPACITY		4 MJ
MGU-K MAXIMUM POWER		120 kW (163 cv)
MGU-K MAXIMUM RPM		50,000
MGU-H MAXIMUM RPM		125,000

Figure 62: Ferrari F1-75's Engine

ANNEX II

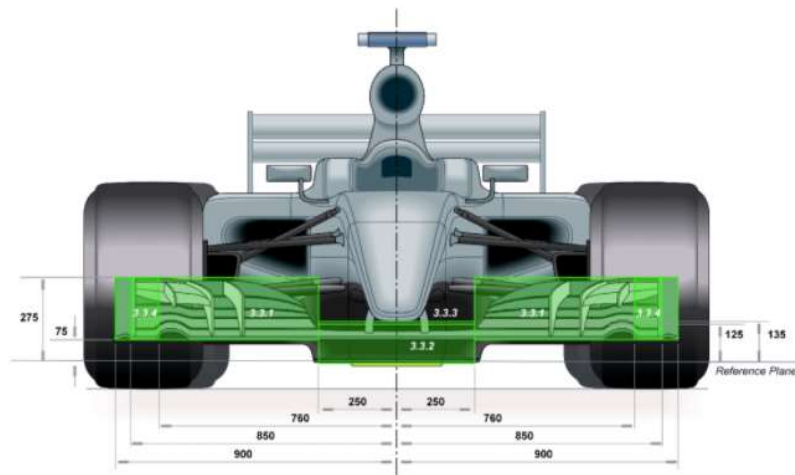


Figure 63: Front View Front Wing Measurements

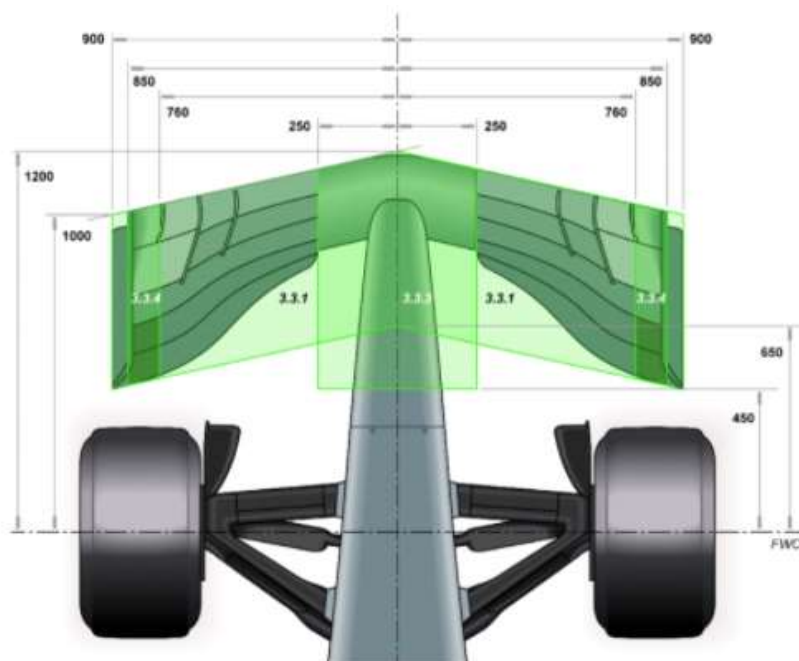


Figure 64: Top View Front Wing Measurements